Available online at www.sciencedirect.com
SCIENCE DIRECT®
Coordination Chemistry Reviews 249 (2005) 1221–1248
COORDINATION CHEMISTRY REVIEWS
www.elsevier.com/locate/ccr

Review

Groups 2 and 3 metal complexes incorporating fluorenyl ligands

Evgueni Kirillov[a], Jean-Yves Saillard[b], Jean-François Carpentier[a,*]

[a] *Organométalliques et Catalyse, UMR 6509, CNRS, Université de Rennes 1, Institut de Chimie de Rennes, Campus de Beaulieu, 35042 Rennes Cedex, France*
[b] *Chimie du Solide et Inorganique Moléculaire, UMR 6511, CNRS, Université de Rennes 1, Institut de Chimie de Rennes, 35042 Rennes Cedex, France*

Received 27 October 2004; accepted 22 January 2005
Available online 2 March 2005

Contents

Abstract

The panorama of fluorenyl complexes of alkaline earth and rare-earth metals is considered. The coordination facilities and bonding abilities of the fluorenyl ligand, common and less usual synthetic procedures of fluorenyl-based metallocenes of groups 2 and 3 elements, as well as applications derived from these fluorenyl complexes in polymerization and organic catalysis are discussed.

Keywords: Fluorenyl ligands; Metallocenes; Lanthanides; Alkaline earth metals; Synthesis; Structure; Homogeneous catalysis

* Corresponding author. Tel.: +33 223 235 950; fax: +33 223 236 939.
E-mail address: jean-francois.carpentier@univ-rennes1.fr (J.-F. Carpentier).

0010-8545/$ – see front matter © 2005 Elsevier B.V. All rights reserved.
doi:10.1016/j.ccr.2005.01.011

1. Introduction

The introduction of fluorenyl ligands in the coordination chemistry of early transition elements has opened up a rich domain of investigation, which has proven especially valuable for the polymerization catalysis field. As reviewed by Alt and Samuel, group 4 metallocenes incorporating various fluorenyl-based ligands represent a unique class of complexes that afford astonishing catalytic activities in the polymerization of ethylene and α-olefins [1]. The fluorenyl moiety can impart exceptional syndiospecific control in propylene polymerization mediated by *ansa*-metallocenes [2], an ability that has initiated a strong interest into sandwich complexes bearing sterically expansive substituted fluorenyl ligands [3]. The use of fluorenyl ligands with alkaline earth and rare-earth metals is more recent, but the work achieved over the past decade has revealed a much more diverse coordination chemistry of fluorenyl-based ligands than so far envisioned with group 4 metals. π-Complexes of early elements and lanthanides are highly ionic by nature and can be considered as isoelectronic d^0 species. As a consequence, the latter can feature very similar, original bonding and structural properties and reactivity.

This review focuses on important structural aspects of fluorenyl complexes of groups 2 and 3 metals, and describes as well the main synthetic problems encountered in their preparation and catalytic applications that have been developed thereof. Accordingly, the review is divided into four main sections. Section 2 discusses the structural and electronic properties of the fluorenyl anion and the variety of coordination modes of fluorenyl ligands that have been observed in complexes of alkaline earth and rare-earth metals. Sections 3 and 4 cover the methods of preparation and structural features of fluorenyl complexes of divalent metals and trivalent rare-earth elements, respectively. Applications of fluorenyl complexes of these elements in modern homogeneous catalysis are discussed in Section 5.

2. The fluorenyl anion and its diverse bonding facilities

The 14π-electron fluorenyl anion ($C_{13}H_9^-$), like the 6π-electron cyclopentadienyl one, belongs to Huckel $(4n+2)\pi$ aromatic systems. The highly aromatic character of the fluorenyl anion is corroborated by ab initio and density functional theory (DFT) computations described by Schleyer and co-workers [4]. However, $C_{13}H_9^-$ demonstrates lower stability in terms of absolute hardness in the row of anions: fluorenyl < indenyl < cyclopentadienyl [5]. This trend is in agreement with the observed hard accessibility and instability of fluorenyl metal complexes under conditions that proved to be suitable for the cyclopentadienyl analogues. This relative instability is related to the existence of a rather high-lying HOMO [5], as illustrated by the DFT-computed MO diagram of $C_{13}H_9^-$ shown in Fig. 1 [6].

Due to its high energy, this orbital is expected to afford particularly strong interaction with accepting orbitals of an incoming metal moiety. Its localization (Fig. 1) favors bonding of the metal to the bridgehead atom and, to a lesser extent, to the two atoms that connect the C_6 rings. Considering the HOMO and HOMO + 1 both together, the same argument suggests that covalent interactions would favor bonding to atoms of the C_5 ring. From the point of view of coulombic charge interaction, a comparison of the computed carbon Mulliken net charges (Scheme 1) [5], again largely favor bonding to the bridgehead atom, while bonding to the other atoms of the C_5 ring are this time expected to be less favored than that to the outer atoms of the C_6 rings. Nevertheless, with a set of seven occupied π-type orbitals delocalized over its whole carbon skeleton, the fluorenyl anion can in principle coordinate metal atoms by using any of its carbon atoms. The nature and the number of the coordinated atoms will depend on the orbital and electrostatic demand of the metal, but also on the steric and strain conditions the whole molecule is under control.

In this regard, one can distinguish seven limiting coordination modes of the fluorenyl ligand that have been observed in metallocene complexes of groups 2 and 3 metals (Scheme 2). The bonding in **A** is reminiscent of "classic" metallocene architectures. Within the framework of a covalent bonding scheme, $C_{13}H_9^-$ behaves in **A** as a 6-electron donor, as well as in **E**. In **B**, **C** and **F**, $C_{13}H_9^-$ is a 4-electron donor. It is a 2-electron donor in **D**, while the situation in **G** cannot be discriminated between $C_{13}H_9^-$ being a 2- or a 4-electron ligand. However, ionic (coulombic) interactions can also be determinant in the choice of the coordination mode for highly electropositive metals such as those of group 3, and particularly of group 2.

3. Fluorenyl complexes of group 2 metals and related divalent lanthanides

Fluorenyl complexes of group 2 metals and divalent lanthanides (namely Sm, Yb) can be surveyed in one section due to the striking similarity of their physicochemical properties and structural features. Two pairs of these metals can be marked out: Ca(II)/Yb(II) and Sr(II)/Sm(II). The near identities of ionic radii of these metals (Ca^{2+} 1.00 Å; Yb^{2+} 1.02 Å and Sr^{2+} 1.21 Å; Sm^{2+} 1.22 Å) [7] make their isoleptic complexes feature structural isomorphism [8], and comparable IR and NMR spectral data suggest similarity in bonding. Their reactivity can be very similar as well [9].

The general synthetic methods of this group of metallocenes incorporating divalent metals are reminiscent of those known for "classic" cyclopentadienyl complexes and include the usual salt metathesis approach, σ-bond metathesis routes

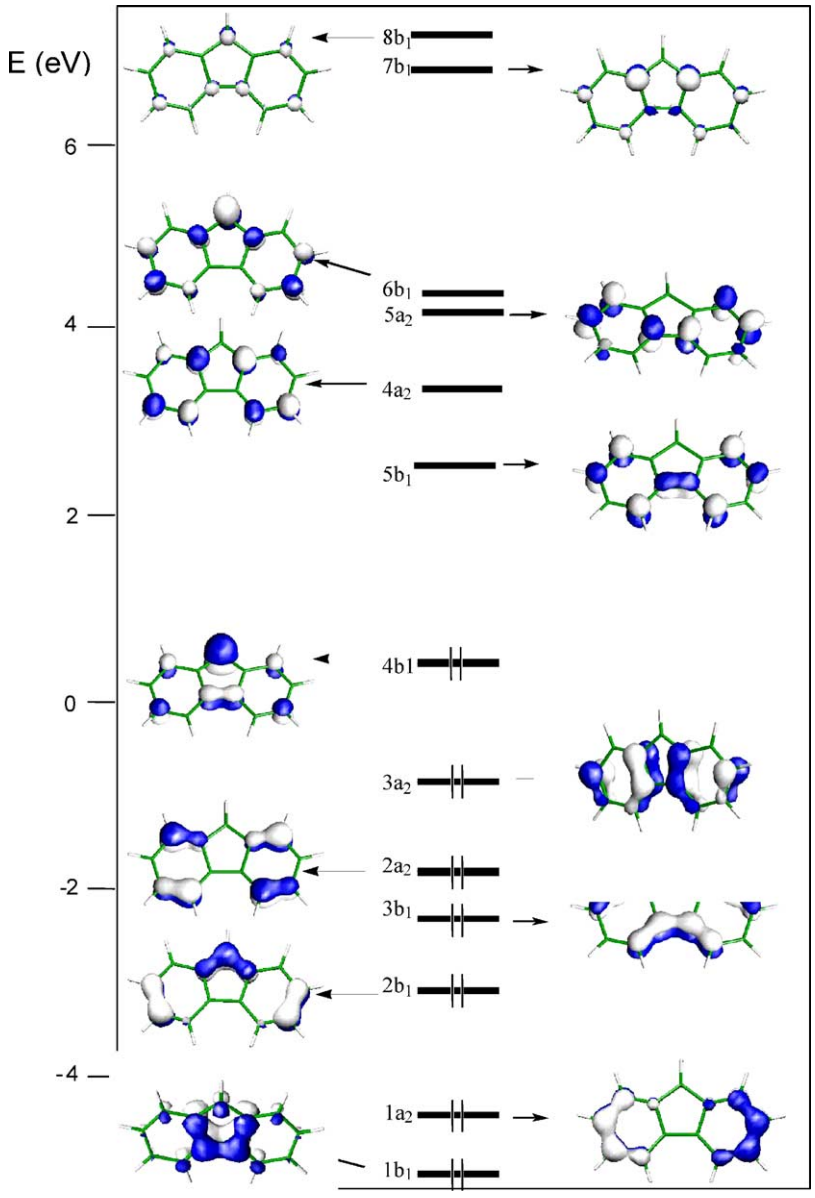

Fig. 1. Molecular π orbital diagram of the fluorenyl anion.

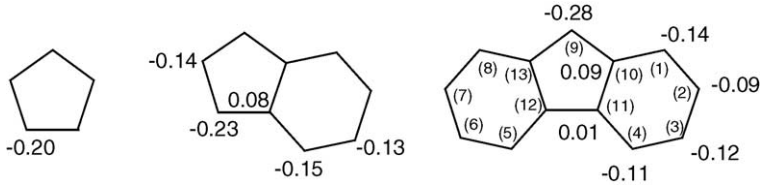

Scheme 1. Calculated Mulliken net charges for the cyclopentadienyl, indenyl and fluorenyl anions [5]. Data in parentheses correspond to the numbering of fluorenyl systems.

(alkane and amine elimination) and even direct deprotonation reactions.

The last method was successfully applied in the late 1960s to the synthesis of the first examples of fluorenyl complexes of alkaline earth metals. A bis(fluorenyl)-barium complex, tentatively formulated "$(C_{13}H_9)_2Ba(ether)_n$" (**1**), was quantitatively prepared upon stirring fluorene in THF on a barium mirror [10]. Alternatively, complex **1** and its strontium analogue were obtained by deprotonation of fluorene in THF or DME with the corresponding metals in the presence of 1,1-diphenylethylene [11,12]. On the basis of variable temperature UV spectroscopic investigations, an ion-paired sandwich structure was attributed to these salts.

The first structurally characterized example of a fluorenyl-barium complex was obtained by Schleyer and co-workers upon reacting fluorene with barium metal (2:1) in liquid ammonia at −80 °C [13]. Subsequent recrystallization of the crude material from THF afforded $(C_{13}H_9)_2Ba(NH_3)_4$ (**2**) (Fig. 2). Interestingly, despite this recrystallization procedure in THF, the barium metal in **2** coordinates exclusively to ammonia molecules. This probably stems from the steric congestion in the equatorial wedge between the fluorenyl planes that favors the coordination of small donor ligands. Two independent conformers in the solid-state structure of **2** were revealed by X-ray diffraction and only one is presented in Fig. 2. The major difference between the two conformers is the manner the fluorenyl ligand coordinates to the metal center: In one conformer, the barium center exhibits nearly symmetric interactions with both five-membered rings of the two fluorenyl moieties (type **A** in Scheme 2), whilst in the other conformer, one fluorenyl moiety is still η^5-bonded, whereas the second fluorenyl ligand is just about to be η^3-coordinated (type **B**). The existence in the same crystal of two different bonding modes has been attributed to a very shallow potential energy surface for the interaction of the metal cation with the fluorenyl anion [13]. A mechanical electron counting for these two conformers would lead to 20 and 18 electrons, respectively. It is likely

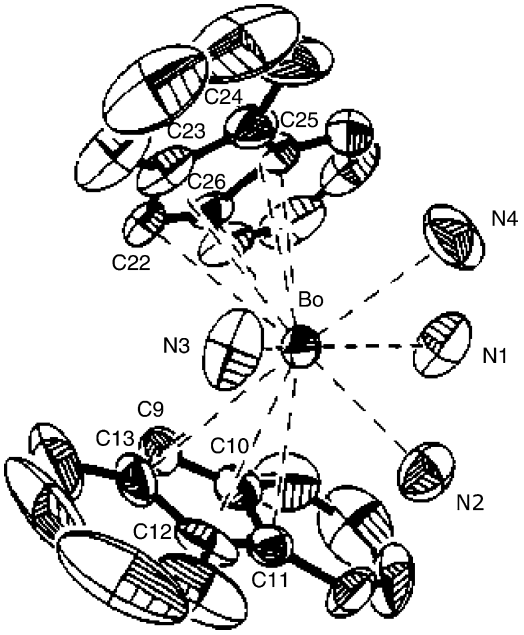

Fig. 2. The crystal structure of complex **2** (only one conformer is shown). Reprinted with permission from Ref. [13]. Copyright 1992 American Chemical Society.

that in these hypervalent (and hypercoordinated) molecules, some of the combinations of the ligand-donating orbitals are non-bonding. Some weak participation of the barium 5d orbitals has been also suggested [13]. Ionic interactions should also play an important role in the bonding of this type of compound.

Since the most common divalent precursors for the salt metathesis reaction are metal iodides, the use of fluorenyl potassium salts is strictly preferable to facilitate the isolation of the target compounds from alkali metal halides. In this regard, the Schlosser *n*-BuLi/KOR superbases [14] are prevalent powerful deprotonating agents.

Non-substituted bis(fluorenyl)samarocene, $(C_{13}H_9)_2Sm(THF)_2$ (**3**), was easily prepared from $SmI_2(THF)_2$ and a

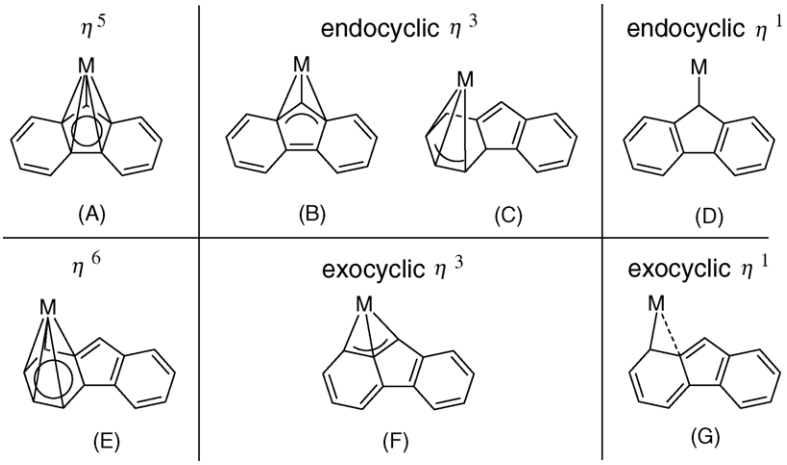

Scheme 2. Coordination modes of fluorenyl ligands observed with groups 2 and 3 metals.

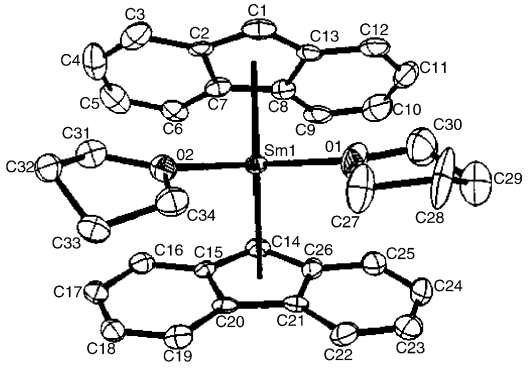

Fig. 3. The crystal structure of complex **3**. Reprinted with permission from Ref. [15]. Copyright 1994 American Chemical Society.

two-fold excess of fluorenyl-potassium in THF [15]. The molecular structure of this complex (Fig. 3) features two inequivalently coordinated fluorenyl ligands as for one conformer of **2**. While one fluorenyl moiety is symmetrically η^5-bonded to the metal center (type **A**), the second ring tends towards a η^3-coordination mode (type **B**). From the considerations discussed in Section 2 and concerning the $C_{13}H_9^-$ HOMO and atomic charge distribution, one may keep in mind that, among the atoms of the C_5 ring, the bridgehead one is somewhat "privileged" for bonding to metal. It follows that the η^5 bonding type **A** will tend to dissymmetrize with a shorter M-bridgehead bond. This distortion towards the η^3 bonding type **B** can make the distinction between η^5 (**A**) and η^3 (**B**) unclear. Depending on whether the second fluorenyl unit in **3** is considered being η^5- or η^3-coordinated, **3** is a 16- or 14-electron complex. The former bonding description makes **3** an isolobal analogue to a very large family of stable 16-electron compounds of the general type Cp_2ML_2 ($M = d^0$) [16], e.g. the numerous bis(fluorenyl)zirconocenes of general formula $(Flu)_2ZrX_2$ (Flu = substituted or unsubstituted fluorenyl ligand; X = halide, amido, alkyl ligand) [1].

The fluorenyl-based ytterbocene $(C_{13}H_9)_2Yb(THF)_2$ (**4**) was synthesized in high yield upon using both the standard salt metathesis approach and substitution method, which involves the reaction of naphthalene–ytterbium with *proteo* fluorene (Scheme 3) [17]. Complex **4** is easily converted to the DME-adduct $(C_{13}H_9)_2Yb(DME)$ (**5**) upon recrystallization from neat dimethoxyethane.

The combined metathesis/substitution procedure between the mixed iodo-naphthalene ytterbium compound, fluorenyl-potassium and pentamethylcyclopentadiene led to the isolation of the mixed-ligand ytterbocene $(C_{13}H_9)(C_5Me_5)Yb(DME)$ (**6**) (Scheme 4).

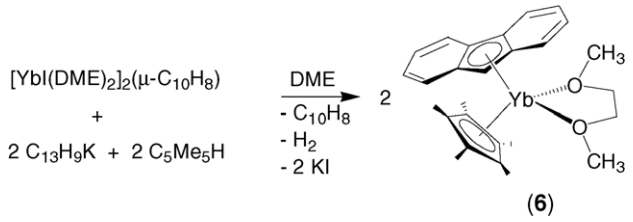

Scheme 4.

The X-ray diffraction analyses carried out for **4** and **6** (Fig. 4a and b) revealed that, in the solid-state structures of both complexes, the fluorenyl ligands are coordinated in a nearly symmetric η^5-fashion, although the moderate ring slippage of 0.25–0.38 Å indicates a tendency to a reduced η^3-mode (type **B**). These observations were related to the relatively small ionic radius of Yb^{2+} [7], which results in consequent steric hindrance of the bulky fluorenyl ligands. We suggest that the major reason of this slippage is rather of electronic origin as discussed above for compound **3** (vide supra).

Complex **4** can be quantitatively oxidized with 1,4-di-*tert*-butyl-diimine to yield the corresponding ytterbocene(III) incorporating the radical-anion diimine ligand (**7**) (Scheme 5) [17]. Quite different products were obtained upon treatment of **4** with bulkier aromatic diimines under the same conditions (Scheme 5) [18]. Thus, an unexpected C–C coupling reaction between ytterbocene **4** and 1,4-bis(di-*iso*-propyl)-diimine without oxidation of the metal was demonstrated, leading eventually to complex **8**. Also, the analogous reaction of 1,4-bis(di-*iso*-propyl)-2,3-dimethyl-diimine with **4** exhibits diverse C–H bond activation pathways, giving the half-sandwich Yb(II) complex **9** with concomitant elimination of *proteo* fluorene.

The crystal structures of both compounds **8** and **9** (Fig. 5a and b) feature quite different coordination modes of the fluorenyl moieties onto ytterbium. Whereas the bonding mode of fluorene in **9** is usual, showing moderate slippage towards η^3 in accord with type **B**, the uncommon open-sandwich coordination environment of the metal in **8** presents two fluorenyl fragment bonded in an exocyclic manner (type **F**).

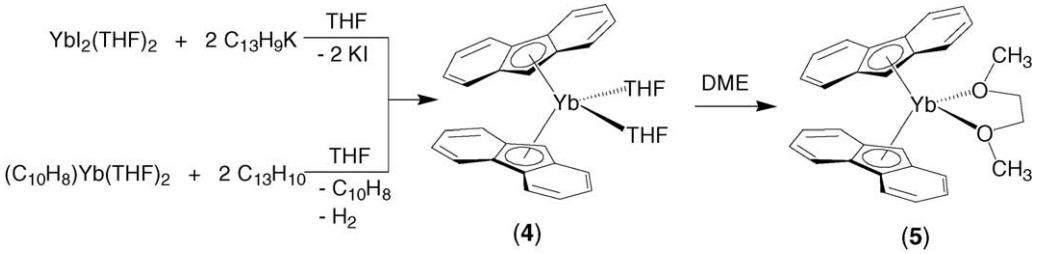

Scheme 3.

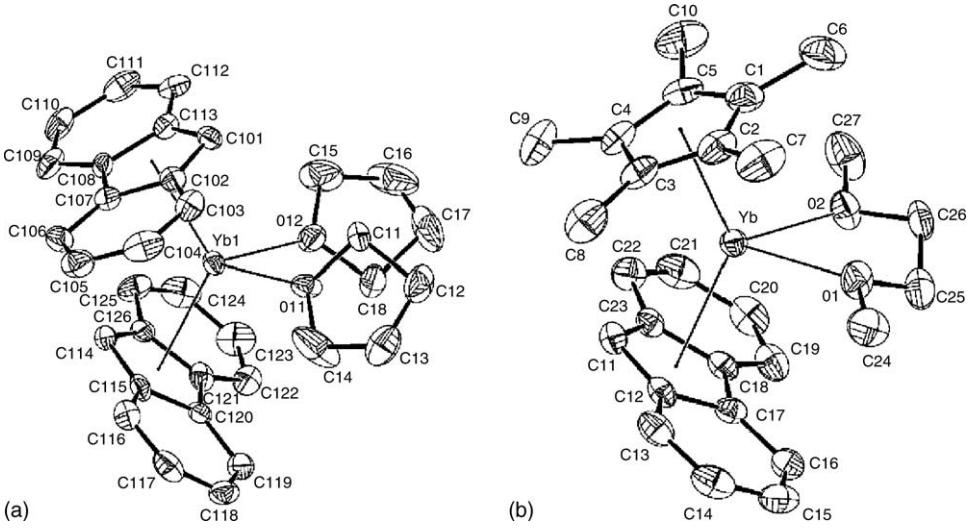

Fig. 4. The crystal structures of complexes **4** (a) and **6** (b). Reprinted with permission from Ref. [17]. Copyright 2001 Wiley.

Also, *ansa*-metallocenes of the divalent ytterbium and samarium metals were prepared by salt metathesis and characterized by ^{1}H and ^{13}C NMR spectroscopy (Scheme 6) [17].

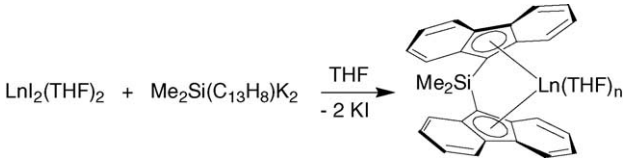

Scheme 6.

Bulky trimethylsilyl-substituted fluorenyl ligands were successfully introduced in the chemistry of divalent organolanthanides by Yasuda and co-workers. Divalent samarium and ytterbium complexes incorporat-

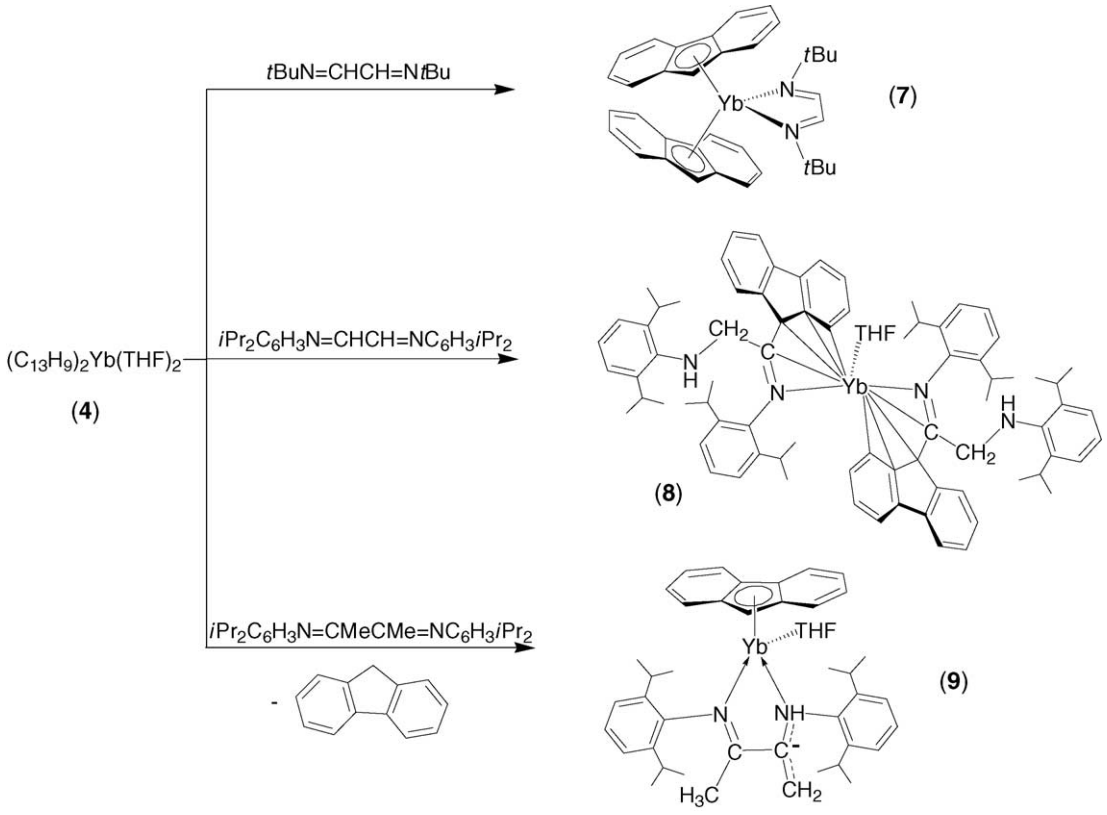

Scheme 5.

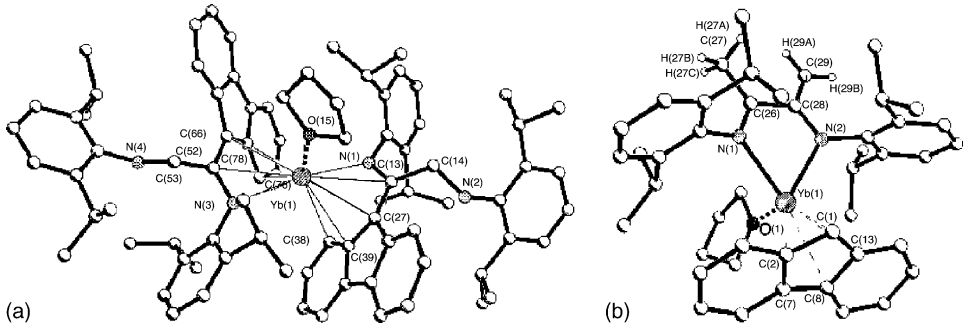

Fig. 5. The crystal structures of complexes **8** (a) and **9** (b). Reprinted with permission from Ref. [18]. Copyright 2004 Wiley.

ing the trimethylsilyl-substituted fluorene ligand (9-Me_3Si–$C_{13}H_8$)$_2$M(THF)$_2$ (M = Sm (**10**), Yb (**11**)) were isolated in good yields from the reaction of the fluorenylpotassium salt with lanthanide iodide in THF [19]. The crystal structure of **10** was determined by X-ray diffraction (Fig. 6). The geometry of this complex resembles that described for **3**, although it demonstrates almost equal participation of all five carbons from the central rings of both the fluorenyl ligands in binding with the samarium center (type **A**). This observation supports our electronic arguments about the difficulty to discriminate between coordination types **A** and **B**, associated with the suggestion of Schleyer and co-workers of a smooth energy profile connecting both types of coordination [13].

Addition of trialkylaluminum derivatives revealed a very unusual reactivity of compounds **10** and **11**. Treatment of the samarium metallocene **10** with a five-fold excess of Me_3Al or Et_3Al resulted in the isolation of heterotrimetallic complexes (9-Me_3Si–$C_{13}H_8$–9′-AlR_3)$_2$Sm (R = Me (**12**), Et) (Scheme 7). The consistency of both products was established by X-ray diffraction analysis and the solid-state structure of the Me_3Al-adduct is presented in Fig. 7a. Formally, complex **12** can be considered as the substitution product by an $AlMe_3$ moiety of the samarium metal center, the latter being shifted, without change in its oxidation state, from the central 5-membered ring to the six-membered ring in an η^6-coordination mode, also called "arene" type (type **E**). The trialkylaluminum moiety is σ-bonded to the fluorenyl ligand and features a bridging agostic interaction by one of the three alkyl groups with the samarium center. Taking into account the agostic bonds, **12** is also a 16-electron complex isoelectronic to Cp_2ZrCl_2.

Similar reactivity of **10** towards other organoaluminum and organoboron derivatives was observed, yielding products of presumably identical structure as judged by NMR. Noteworthy, those heterotrimetallic complexes can be reversibly converted to the parent samarocene **10** upon addition of THF (Scheme 7).

Surprisingly, two different products were obtained upon treatment of the ytterbocene **11** with excess Me_3Al [19]. The first one is the heterobimetallic complex of Yb(II) (9-Me_3Si–$C_{13}H_8$–9′-$AlMe_3$)Yb(Me_3Si–$C_{13}H_8$) (**13**), which is composed of two non-equivalent fluorenyl ligands (Fig. 7b): one remains symmetrically η^5-bound to ytterbium (type **A**), whereas the coordination of the second ligand is the same

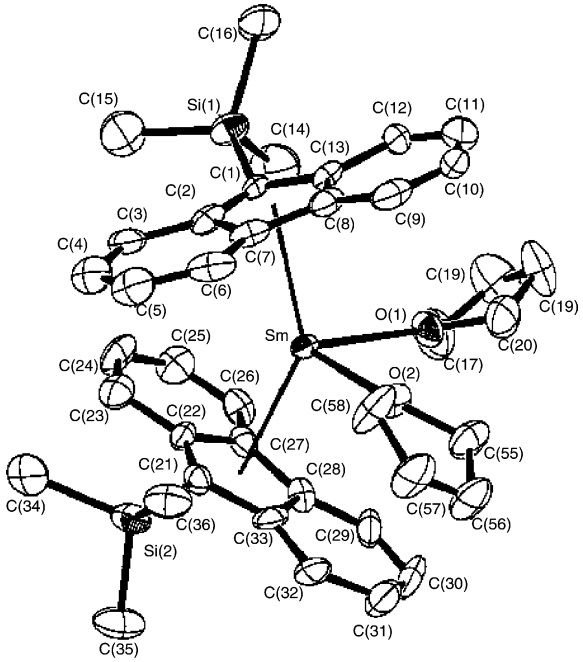

Fig. 6. The crystal structure of complex **10**. Reprinted with permission from Ref. [19]. Copyright 2000 American Chemical Society.

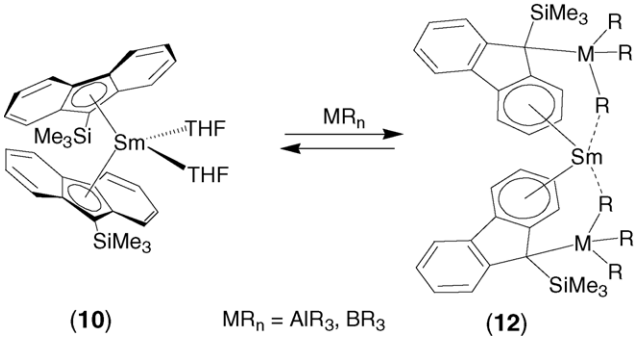

Scheme 7.

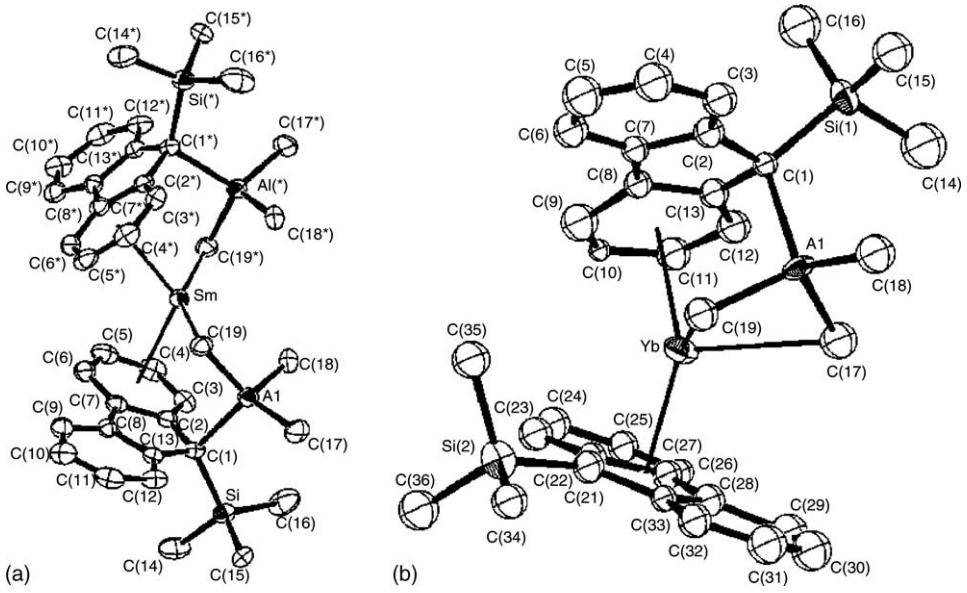

Fig. 7. The crystal structures of complexes **12** (a) and **13** (b). Reprinted with permission from Ref. [19]. Copyright 2000 American Chemical Society.

(η^6, type **E**) as the one described for the aforementioned samarium complex **12**. Also, complex **13** features agostic interactions of the bridging Me_3Al unit with the metal center via two methyl groups at the same time. The second product isolated from this reaction is the fully dissociated ion pair $[(C_{13}H_9)Yb(THF)_4]^+[AlMe_4]^-$ (**14**) in which the cation is presented by a half-sandwich, non-substituted fluorenyl-ytterbium tetrakis-THF-adduct (Fig. 8) that shows the "classic" coordination of the fluorenyl moiety (type **A**). Complex **14** is a 14-electron species related to other piano-stool $CpML_4$ moieties [20]. The formation of the mono-trimethylaluminum adduct **13** instead of heterotrimetallic complex similar to **12** can be reasonably ascribed to the smaller ionic radius of ytterbium and steric considerations that derive thereof. However, the pathway to the second complex (**14**), in particular how the trimethylsilyl moiety is removed from fluorenyl, remains unclear.

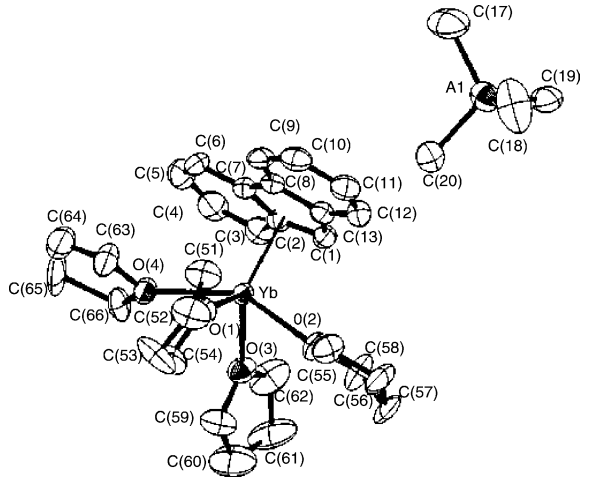

Fig. 8. The crystal structure of complex **14**. Reprinted with permission from Ref. [19]. Copyright 2000 American Chemical Society.

The mono-THF adduct of divalent ytterbocene (9-Me_3Si–$C_{13}H_8)_2Yb(THF)$ (**15**) was obtained from the reaction of fluorenyl-sodium with ytterbium diiodide and used next for the preparation of the bimetallic species (9-Me_3Si–$C_{13}H_8)_2YbAlH_3(NEt_3)$ (**16**) by treatment of **15** with alane (aluminum trihydride) [21,22]. The identity of both complexes was established by NMR spectroscopy but no structural identification was reported, so that the actual coordination mode of the fluorenyl ligands remains unknown.

The chemistry of alkaline-earth complexes incorporating a series of bulky silicon-substituted fluorenyl ligands was intensively investigated by Harder et al. For instance, the reaction between 2 equiv. of 9-Me_3Si–$C_{13}H_8K$ and CaI_2 was shown to proceed smoothly in THF to give (9-Me_3Si–$C_{13}H_8)_2Ca(THF)_2$ (**17**) [23]. Recrystallization of **17** from benzene in the presence of a small amount of THF gave surprisingly the ion-paired derivative $[9\text{-}Me_3Si\text{–}C_{13}H_8^-]_2[Ca^{2+}(THF)_6]\cdot C_6H_6$ (**18**) (Fig. 9a). The octahedral coordination of the calcium atom by six THF molecules apparently prevents bonding of the fluorenyl anions, which are equidistant from the metal center and parallel to each other. The whole molecule interacts with two neighboring molecules, which results in a two-dimensional coordination polymer. Also, the α-protons of the coordinated THF molecules appear in close contacts with the π-clouds of the six-membered rings of the fluorenyl anions and encapsulated benzene molecule as well (Fig. 9b). The shortest C–H···π contact was found to be 2.615 Å, which is shorter than or close to the sum of the van der Waal's radii of the carbon and hydrogen atoms.

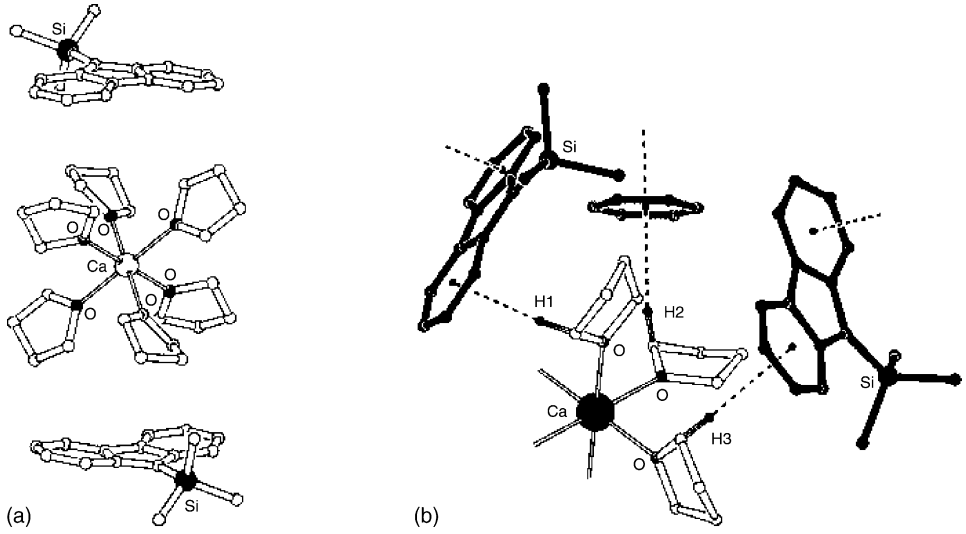

Fig. 9. The crystal structure of complex **18** (a) and C—H···ring$_{cent}$ interactions in complex **18** (b). Reprinted with permission from Ref. [23]. Copyright 2002 Wiley.

This highly self-organized structure is retained in benzene/THF solution, as confirmed by 2D ROESY ^{1}H NMR experiments. Partial loss of coordinated THF molecules occurs in pure benzene solution, which is presumably accompanied by the transformation of dicationic **18** to a neutral metallocene (**17**) through an intermediate mono-cationic species (Scheme 8).

The isostructural magnesium and ytterbium complexes [9-Me_3Si–$C_{13}H_8^-$]$_2$ [M^{2+}(THF)$_6$] C_6H_6 (M = Mg, **19** [23]; M = Yb, (**20**) [24]) were synthesized similarly from 9-Me_3Si–$C_{13}H_8K$ and the metal dihalogenides and crystallized from THF/benzene mixture.

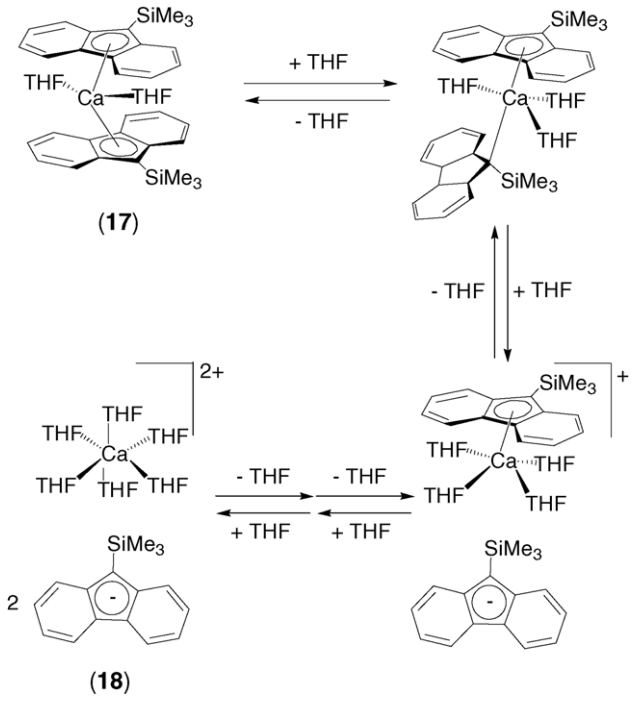

Scheme 8.

Bulky 9-substituted hypersilyl fluorenyl complexes of calcium and strontium (9-(Me_3Si)$_3$Si–$C_{13}H_8$)$_2$M(THF)$_2$ (M = Ca (**21**), Sr (**22**)) were obtained in good yields from the reaction between MI_2 and a two-fold excess of 9-(Me_3Si)$_3$Si–$C_{13}H_8$K [25]. The crystal structures of both complexes (Fig. 10) feature close structural similarities, e.g., the both compounds are bis-THF adducts and the coordination mode of one of the two fluorenyl ligands in these complexes is symmetric η^5 (type **A**). However, the coordination of the second fluorenyl ligand is quite unusual and differs in both crystal structures: in the calcium complex **21**, this moiety is unsymmetrically η^3-bonded to the metal with the outer edge of one of the six-membered rings (type **C**), whilst the strontium analogue **22** features nearly symmetric η^6 "arene" coordination of the second fluorenyl moiety (type **E**). The reason for the coordination of the second fluorenyl ligand to the metal center by the peripheral π-systems of the benzene rings was proposed to arise from enormous steric congestion provided by the bulky hypersilyl substituents. This appears to be severe in the case of the calcium compound, inducing extrusion of the second fluorenyl ligand from the coordination sphere. In the case of the strontium analogue, the larger coordination sphere of the metal with larger ionic radius makes possible the second fluorenyl ligand to bind more effectively in an η^6-manner. These steric considerations are in agreement with the observation that the (Me_3Si)$_3$Si groups are significantly bent out (10–20°) of the C_5 plane away from the metal both in **21** and **22**.

Analogously, alkaline earth metal compounds bearing the uncommon 1,2-bis(dimethylamino)-1,2-di-9-fluorenyldiborate ligand were synthesized by reacting the disodium salt of the latter with metal bromides in THF [26]. Hetero-*ansa*-bridged complexes [Me_2NB(9-

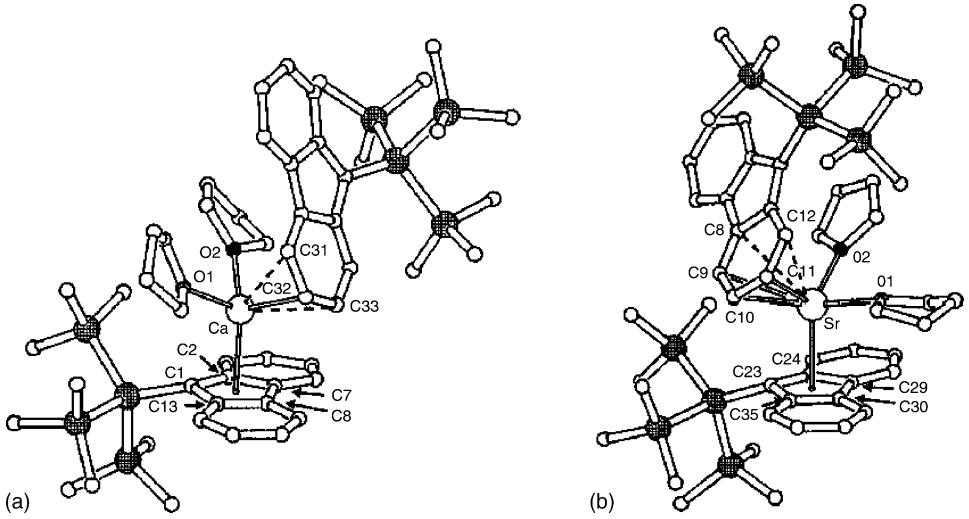

Fig. 10. The crystal structures of complexes **21** (a) and **22** (b). Reprinted with permission from Ref. [25]. Copyright 2003 Wiley.

$C_{13}H_8)]_2M(THF)_2$ of Mg, Ca (**23**) and Ba were isolated in good yields. The solid-state structure of the calcium derivative was established by X-ray analysis (Fig. 11). The fluorenyl fragments are nearly equivalent, displaying an η^5-coordination mode (type **A**) tending toward reduced η^3-hapticity.

Alternative to salt metathesis, a σ-bond metathesis route, i.e. amine elimination, was used as a convenient synthetic approach toward group 2 metal derivatives. For example, the calcium and barium *ansa*-metallocenes $\{Me_2Si(9\text{-}C_{13}H_8)_2\}M(THF)_n$ (Ca (**24**), $n = 3$; Ba (**25**), $n = 4$) were obtained from the direct reaction of the corresponding bis(trimethylsilyl)amide metal precursors and *diproteo* bis(fluorenyl)dimethylsilane (Scheme 9) [27].

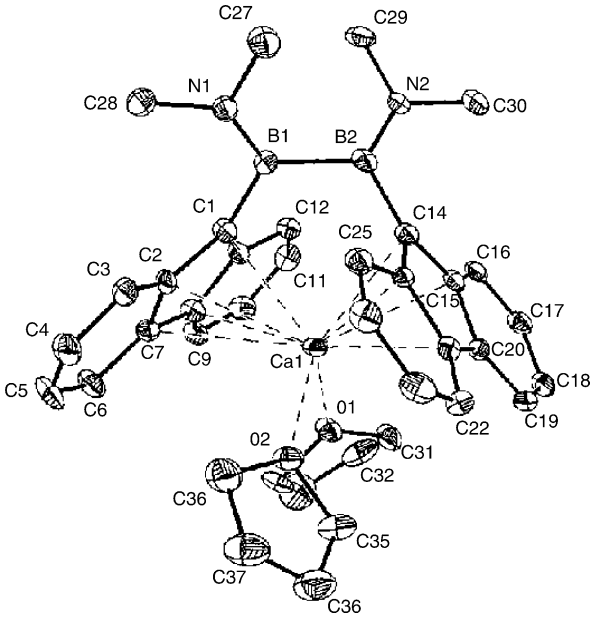

Fig. 11. The crystal structure of the calcium complex **23**. Reprinted with permission from Ref. [26]. Copyright 1994 Wiley.

The molecular structures of both compounds were established by X-ray diffraction studies (Fig. 12). As expected from the differences in ionic radii of the metals, complexes **24** and **25** feature diverse coordination abilities, e.g., the calcium complex is a tris-THF adduct, whereas the barium analogue is a tetrakis-THF solvate. The unit cell of **25** contains two independent molecules that differ in the coordination mode of the fluorenyl ligand. One features the bidentate bis(fluorenyl) ligand bound to barium via a distorted η^5-coordinated fluorenyl moiety (type **A**) and an exocyclic η^3-mode for the second fluorenyl fragment (type **F**) (Fig. 12b). The second molecule in **25** shows double exocyclic η^3-coordination of both fluorenyl ligands (type **F**) (Fig. 12c), similar to that observed in the calcium analogue **24** (Fig. 12a). Such unusual type of coordination involves the bridgehead carbon atom of the central ring and the two adjacent carbon atoms of one six-membered ring.

A similar amine elimination approach between calcium and barium amides $M[N(SiMe_3)_2]_2$ and the phosphorus-bridged bis(fluorenyl) ligand $MeP(C_{13}H_9)_2$ was attempted to generate the corresponding metallocenes [28]. Albeit free amine $HN(SiMe_3)_2$ was detected as a product by ^1H NMR, no alkaline earth metal complex could be isolated. Another protocol was used, by reacting $Ca[N(SiMe_3)_2]_2$ with phosphonium iodide $[MeP(C_{13}H_9)_2]I$ in THF to give the ionic complex $[MeP^+(C_{13}H_9)_2]^-[CaI(THF)_5]^+$ (**26**). The barium analogue was obtained similarly. The solid-state structure of

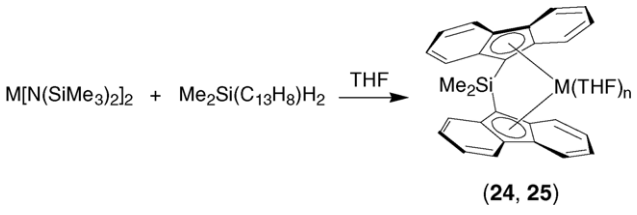

Scheme 9.

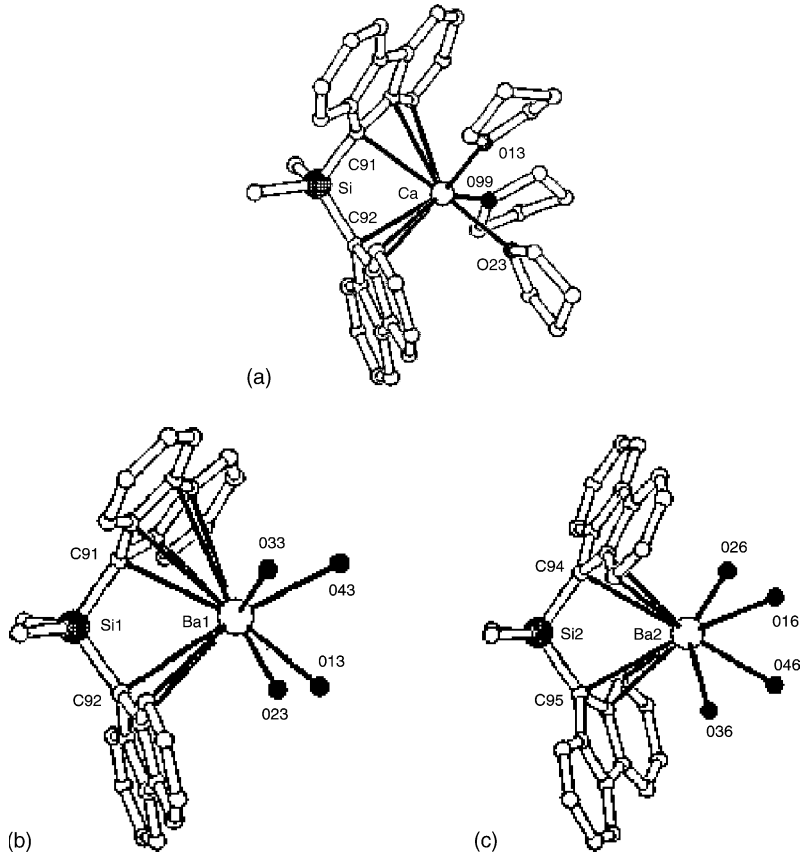

Fig. 12. The crystal structures of complex **24** (a) and the two independent molecules of complex **25** (b, c). Reprinted with permission from Ref. [27]. Copyright 1997 American Chemical Society.

26 consists of discrete six-coordinate THF-solvated calcium mono-iodide cation and phosphonium difluorenylide anion (Fig. 13).

The putative bis(fluorenyl)magnocene $(C_{13}H_8)_2Mg$ was suggested as the product of the σ-bond metathesis reaction between di-*n*-butylmagnesium and *proteo* fluorene [29]. However, neither the solid-state nor the solution structure of the latter was established. Similar fluorenyl magnesium complexes were also prepared via similar alkane elimination starting from polyamine-adducts of dimethylmagnesium and unambiguously characterized [30]. Me_2Mg(TMEDA) reacts in benzene with 1 equiv. of fluorene to give the "neutral" mixed fluorenyl alkyl-magnesium complex $(C_{13}H_9)$MgMe(TMEDA)

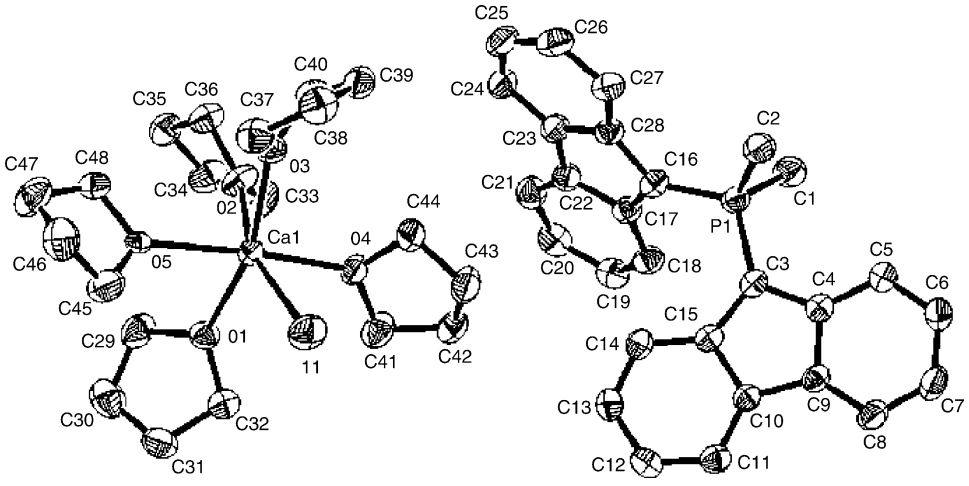

Fig. 13. The crystal structure of complex **26**. Reprinted with permission from Ref. [28]. Copyright 2000 American Chemical Society.

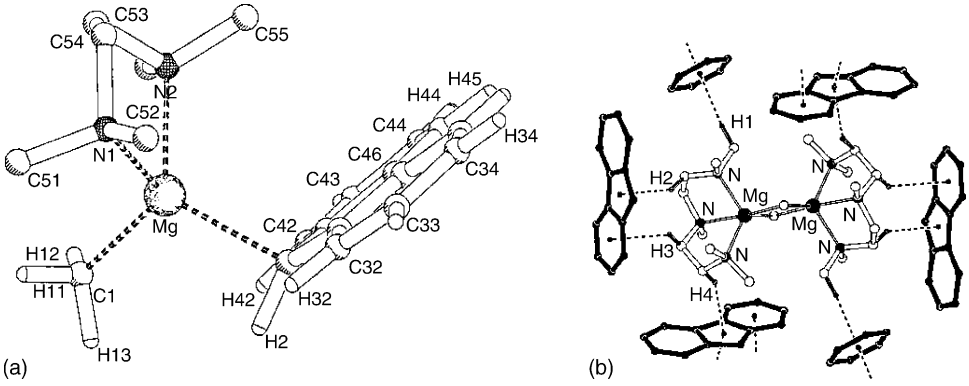

Fig. 14. The crystal structures of complexes **27** (a) and **28** (b). Reprinted with permission from Ref. [30]. Copyright 1994 Wiley.

(**27**). In contrast, the reaction of fluorene with the pentamethylethylenetriamine-adduct Me_2Mg(PMETA) under the same conditions led to solvent-separated dicationic derivative $[Mg_2Me_2(PMETA)]^{2+}[C_{13}H_9^-]_2$ (**28**). The solid-state structure of the "neutral" Grignard-like alkylmagnesium complex **27** clearly features monodentate σ-bonding of the fluorenyl ligand to magnesium via the electron-rich head-on atom (type **D**) (Fig. 14a). Thus the Mg atom is sp^3-hybridized and satisfies the octet rule. This is not the case in the dimeric species **28**, where the coordination sphere of each metal atom is completely saturated with the solvent molecule making the fluorenyl anions moved aside (Fig. 14b). The latter are discrete and do not bond to the magnesium atoms but participate in non-valent close contacts by π-systems of the six- and five-membered rings with the protons of the methylene groups in PMETA donor ligand.

Triphenylmethylcalcium chloride metallates fluorene in THF solution to yield the half-sandwich complex $(C_{13}H_9)CaCl(THF)_2$ (**29**) [31]. The consistency of complex **29** was established by IR and NMR spectroscopies. Also, the hydrolysis of **29** liberates fluorene and its carboxylation yields 9-fluorene-carboxylic acid.

The σ-bond metathesis reaction between homoleptic calcium bis(benzyl) precursors and trimethylsilyl-substituted fluorene proceeded at 25–65 °C in benzene to give half-sandwich calcium complexes (9-Me_3Si–$C_{13}H_8$)Ca(RCH–*o*-C_6H_4–NMe_2)$(THF)_n$ (R = $SiMe_3$ (**30**), $n = 1$ [32]; Me (**31**), $n = 1$ [33]; R = H (**32**), $n = 0$ [34]) (Scheme 10).

The molecular structures of complexes **30**–**32** are shown in Fig. 15. Two of these compounds, namely **30** and **31**, are

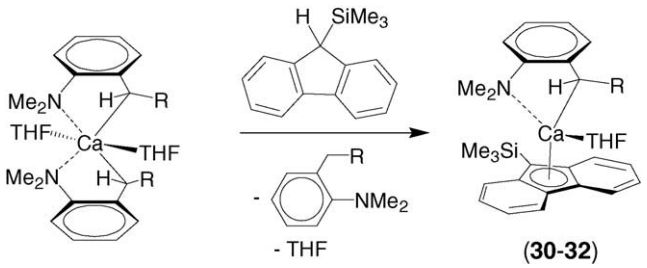

Scheme 10.

monomeric mono-THF adducts, whereas complex **32** exists as a dimer with bridging benzylic carbon atoms. As a consequence, the Ca–C bonds in **32** are slightly elongated (ca. 0.03 Å) as compared to those in **30** and **31**. Obviously, the dimeric structure of **32** arises from the absence of substituent at the benzyl methylene group. The coordination modes of the fluorenyl ligands are very similar in all the three complexes and approach an η^5-mode, with a slight distortion towards an allylic η^3-coordination (type **B**).

The heteroleptic species **30** and **31** retain their composition in solution without any dismutative ligand exchange, as judged by NMR spectroscopy. Fast inversion of the chiral carbanion at benzylic carbon atom takes place in solution upon raising the temperature. The thermodynamic parameters for this process were estimated to be $\Delta G^{\neq} = 18.8$ kcal mol^{-1} for **30** and $\Delta G^{\neq} = 17.2$ kcal mol^{-1} for **31**. Addition of small amounts of THF at room temperature also results in fast inversion of configuration at the chiral center via a THF-assisted bond-breaking process (Scheme 11). Complex **32** preserves its dimeric structure in benzene solution as established by NMR spectroscopy but dissolving it in THF leads to the immediate formation of the dicationic ion-paired derivative **18** [23]. The intermediate for such transformation is likely to be the monomeric THF-adduct (9-Me_3Si–$C_{13}H_8$)Ca(CH_2–*o*-C_6H_4–NMe_2)(THF) that is isostructural to **30** and **31**.

A divalent ytterbium complex analogous to **30**, (9-Me_3Si–$C_{13}H_8$)Yb(Me_3SiCH–*o*-C_6H_4–NMe_2)(THF) (**33**), was prepared via σ-bond metathesis reaction [24]. Although the solid-state structure could not be resolved, the unit cell parameters are comparable to those found for complex **30**. The ^{1}H NMR spectrum of **33** in benzene displays nearly equal chemical shifts to those of **30**, the concentration-independent coalescence temperature and activation energy measured being slightly different ($\Delta G^{\neq} = 17.0$ kcal mol^{-1}) [24].

The unusual product **34** derived from the 9-substituted hypersilyl fluorenyl ligand was obtained in the attempted synthesis of the heteroleptic calcium complex analogous to **30** and **31** (Scheme 12) [33]. No mixed-ligand intermediate could be detected by NMR, indicating that a fast intramolecular C–H activation (or cyclometallation) takes place. The

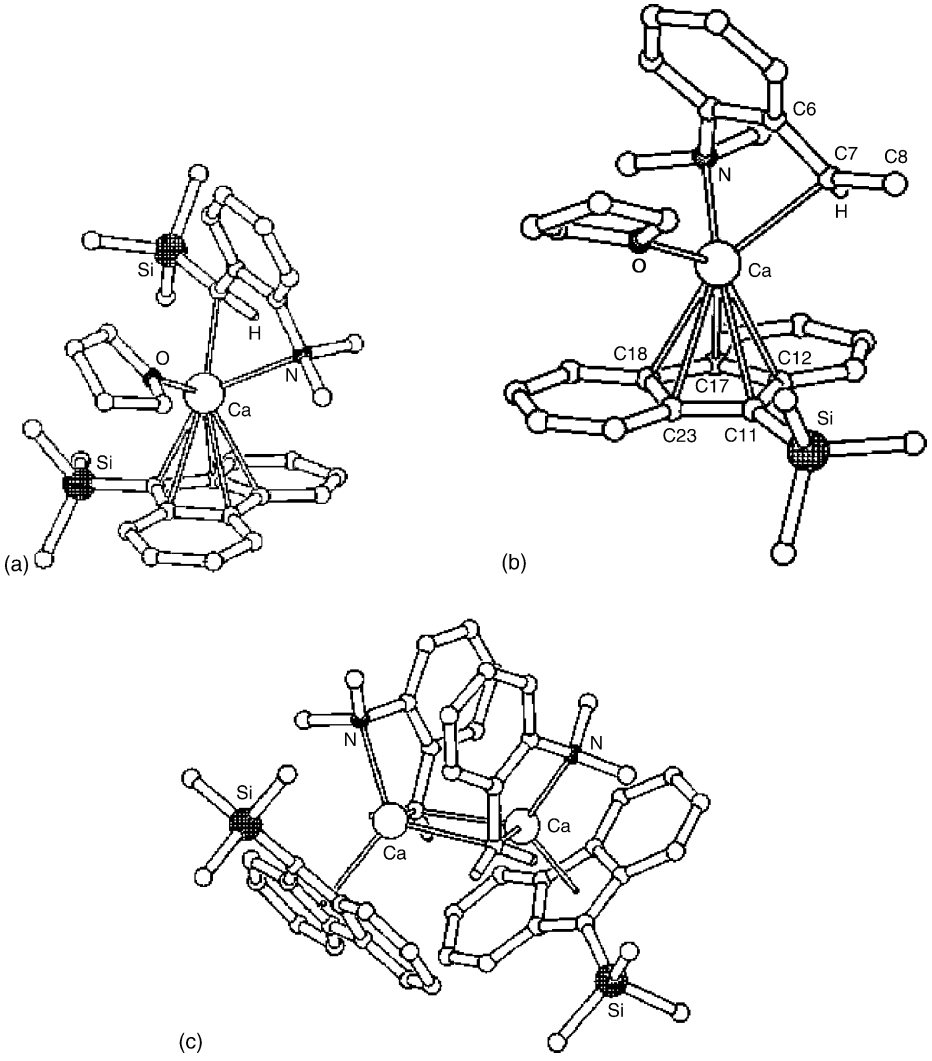

Fig. 15. The crystal structures of complexes **30** (a), **31** (b) and **32** (c). Reprinted with permission from Refs. [32–34]. Copyright 2001 Wiley, Elsevier 2003, American Chemical Society 2002.

X-ray diffraction study revealed that, in the solid state, **34** is a dimer with bridging methylene–silylene groups (Fig. 16). The fluorenyl ligands are equivalent, showing symmetrical η^5-bonding onto calcium (type **A**), but the calcium atoms have a dissimilar coordination sphere. One metal atom binds to a THF molecule, whereas the second metal center displays short interactions to the edge of a fluorenyl ligand. In benzene solution, these inequivalent fluorenyl ligands are in slow exchange, as observed by NMR spectroscopy. Addition of THF results in the formation of the monomeric species.

4. Fluorenyl complexes of trivalent lanthanides and related group 3 metals

Cyclopentadienyl and related complexes of trivalent lanthanides are isoelectronic analogues of group 4 cationic species, which are the real active species in olefin polymerization catalysis. They are, therefore, a strategically important class of materials for modelling complex intermediates and investigating their properties, as well as for developing new single-site catalyst systems. It is thus not surprising that many attempts to prepare group 3 *ansa*-metallocenes of general formula $\{R_2E(Cp^1)(Cp^2)\}Ln(R)$ (Cp^1, Cp^2 = cyclopentadienyl-type fragments; R_2E = linking group (e.g., R_2Si, R_2C); R = alkyl) were undertaken. This section describes three main categories of *ansa*-fluorenyl complexes: (i) Single-carbon bridged *ansa*-metallocenes of lanthanides, which are excellent candidates for polymerization purposes, taking into account that group 4 isoleptic cationic analogues were shown to be among the most active and stereoselective catalysts [2]. (ii) Silylene-bridged *ansa*-metallocenes that feature wider bite angles and are to be compared with ethylene-bridged fluorenyl complexes. (iii) The more recent class of "constrained geometry" half-sandwich complexes incorporating fluorenyl ligands, which is related to a new generation of highly stereospecific catalysts for ethylene and α-olefin polymerization.

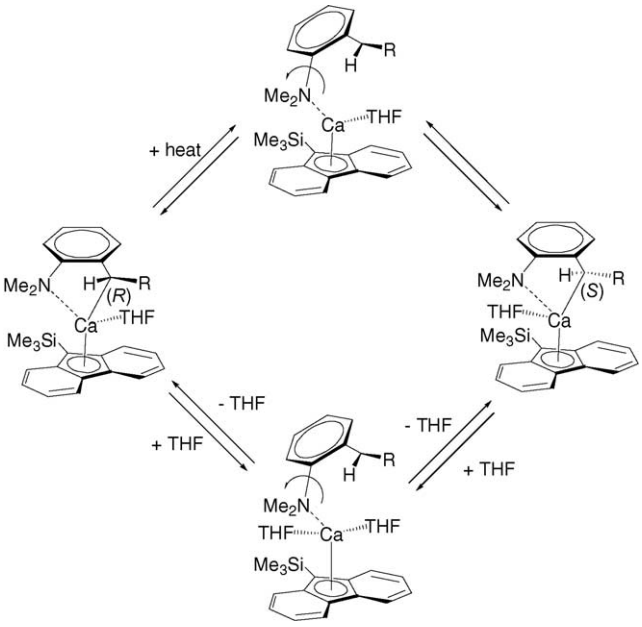

Scheme 11.

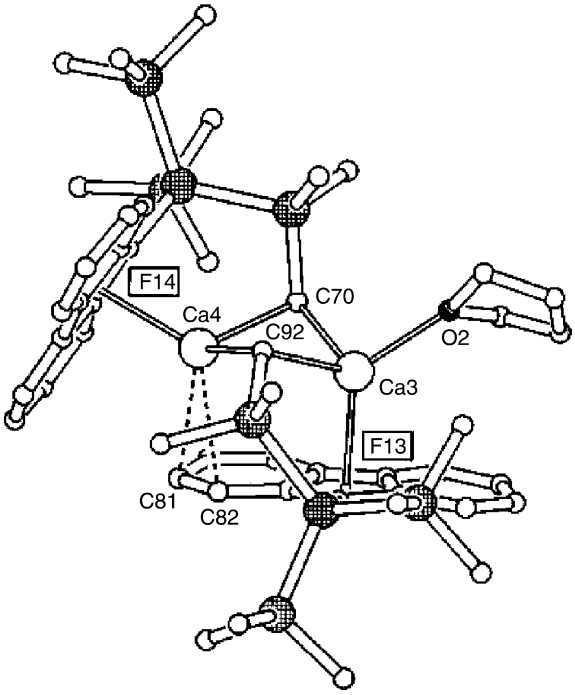

Fig. 16. The crystal structure of complex **34**. Reprinted with permission from Ref. [33]. Copyright 2003 Elsevier.

4.1. Early work on non-bridged half-sandwich complexes

The first fluorenyl organolanthanides $(C_{13}H_9)_2LnCl_2Li(THF)_2$ (Ln = La, Nd, Sm, Ho, Lu) reported by Beletskaya and co-workers in the early 1980s were prepared from fluorenyl-lithium and lanthanide trichlorides in THF [35,36]. These complexes were suggested to have metal–ligand σ-bond on the basis of spectroscopic data. The mono-fluorenyl anionic complex $[(C_{13}H_8)La(C_3H_5)_3]^-[Li(C_4H_8O_2)_2]^+$ (**35**) was isolated in low yield from the reaction of the allyl precursor $[La(C_3H_5)_4]^-[Li(C_4H_8O_2)_2]^+$ with an equimolar amount of *proteo* fluorene [37]. No crystallographic study was carried out, but an η^5-coordination of the fluorenyl moiety onto lanthanum was suggested.

4.2. ansa-Metallocenes bearing carbon-bridged fluorenyl-based ligands

The preparation of trivalent lanthanide species incorporating carbon-bridged fluorenyl-cyclopentadienyl ligands by salt metathesis routes was first developed by Qian et al. Anionic complexes (also called *ate*-complexes) of "small" group 3 elements $[\{Ph_2C(C_{13}H_8)(C_5H_4)\}LnCl_2]^-[Li(THF)_4]^+$ (Ln = Y, **36**; Lu, **37**) bearing a diphenylmethylene-bridged fluorenyl-cyclopentadienyl ligand were prepared by reacting the dilithium salt of the ligand with metal trichlorides [38]. The synthesis of the complexes of larger lanthanides (La, Nd) with this ligand system was successful only when tetraborohydride lanthanide precursors $Ln(BH_4)_3(THF)_n$ (Ln = La, Nd) were used. Thus, the anionic compounds $[\{Ph_2C(C_{13}H_8)(C_5H_4)\}Ln(BH_4)_2]^-[Li(THF)_4]^+$ (Ln = La, **38**; Nd, **39**) and $[\{Ph_2C(C_{13}H_8)(C_5H_4)\}Nd(BH_4)_2]^-[K(18\text{-crown-6})]$ (**40**) were isolated [39]. The structurally characterized **37** and **40** were shown to display comparable geometry and bonding features of the ligand with metal in the solid state (Fig. 17). Both products comprise a fully dissociate alkaline metal cation and lanthanide-based anion, and the latter adopts a pseudotetrahedral coordination environment of the metal center that is observed in a variety of $[Cp_2LnX_2]^-$ anions (which is, as aforementioned, isolobal to the large family of stable 16-electron compounds of the general type Cp_2ML_2 (M = d^0) [16]). The coordination modes

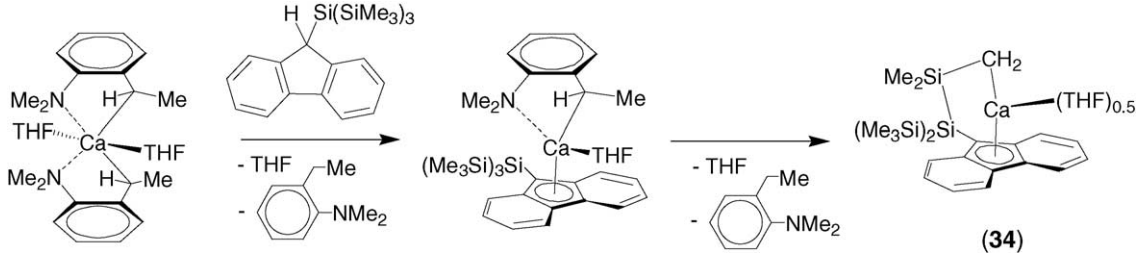

Scheme 12.

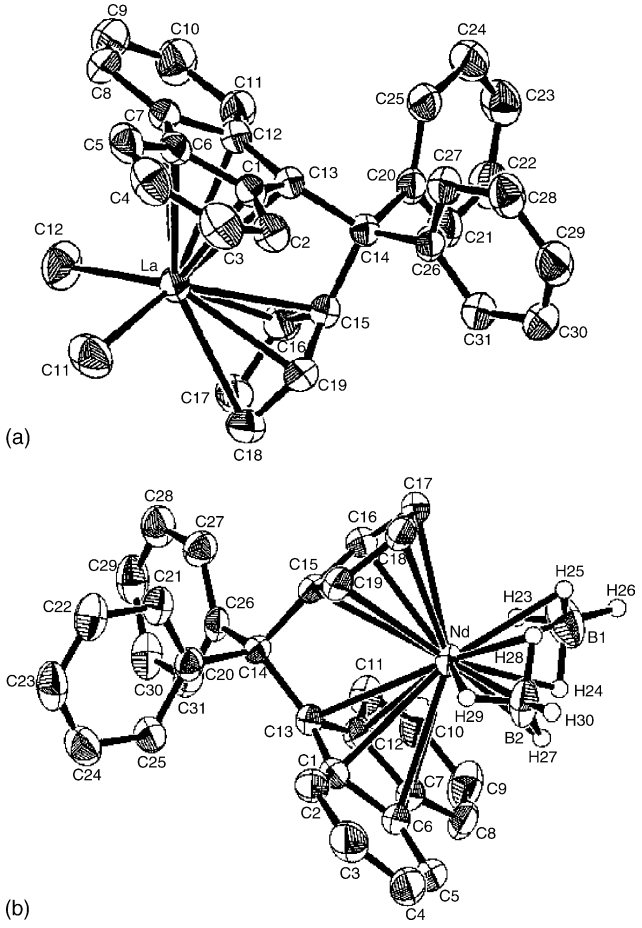

Fig. 17. The crystal structures of the anions of complex **37** (a) and complex **40** (b). Reprinted with permission from Ref. [39]. Copyright 2001 Elsevier.

of the fluorenyl moieties in **37** and **40** are also very similar, that is η^5-bonding (type **A**) with a minor tendency towards a reduced η^3-mode.

Further reaction of the dichloro complex **37** with $KN(SiMe_3)_2$ afforded the "neutral" base-free amido derivative $\{Ph_2C(C_{13}H_8)(C_5H_4)\}Lu[N(SiMe_3)_2]$ (**41**) [40], which features a nearly symmetrically (η^5) coordinated fluorenyl ligand (Fig. 18). The difference in bonding of the fluorenyl ligand in **41**, as compared to that observed in the parent metallocene **37**, was related to the lower steric constrains of a sole amido group relative to two chlorine atoms. Additional stabilization of the complex by agostic interaction of the metal with the carbon atom C(32) was shown from X-ray diffraction data. It allows **41** to achieve the stable 16-electron count of compounds of the general d^0 Cp_2ML_2 type.

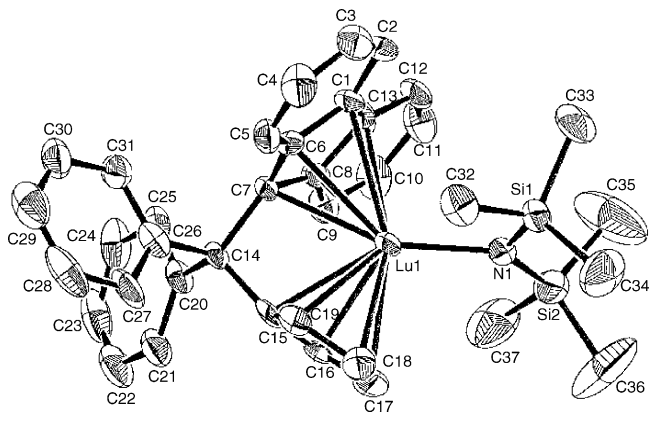

Fig. 18. The molecular structure of complex **41**. Reprinted with permission from Ref. [40]. Copyright 2002 Elsevier.

An alternative entry toward fluorenyl-based lanthanidocene amides via amine elimination was investigated in details from the reaction of lanthanide amides $Ln[N(SiMe_3)_2]_3$ (Ln = Y, La, Nd) with the isopropylidene-bridged ligand $Me_2C(C_{13}H_9)(C_5H_5)$ [41]. The formation of various cyclopentadienyl derivatives that have free hanging fluorene moieties was observed, presumably because of the much lower acidity of the fluorenyl proton as compared to the cyclopentadienyl proton. Thus, the formation of the mono-substituted intermediate **42** was detected by NMR spectroscopy in the reaction between equimolar amounts of *diproteo* ligand and $Y[N(SiMe_3)_2]_3$ in THF at 5 °C (Scheme 13). Subsequent transformation of **42** into the bis(cyclopentadienyl) complex **43** takes place slowly under these conditions and can be accelerated by heating. Unlike the mono-substituted bis(amido) intermediate, **43** appeared to be kinetically more stable and could be isolated and characterized by NMR spectroscopy and an X-ray diffraction study. In solution, **43** progressively converts into tris(cyclopentadienyl) product **44** via further disproportionation. However, upon refluxing in THF and removing of concomitantly formed amine, complex **43** undergoes an intramolecular amine elimination reaction to give *ansa*-metallocene **45** with a pendant fluorenyl arm. This process is reversible as demonstrated by the retroformation of the bis(cyclopentadienyl)amide **43** upon addition of excess of amine $HN(SiMe_3)_2$ to a toluene solution of **45**.

Similar reactivity trends were observed starting from lanthanum and neodymium amides [41]. Using an analogous synthetic protocol, *ansa*-lanthanidocenes $\{Me_2C(C_{13}H_8)(C_5H_4)\}Ln(\eta^5\text{-}\{Me_2C(C_{13}H_9)(C_5H_4)\})(THF)$ (Ln = La, **46**; Nd, **47**) were prepared in good yields. X-ray diffraction studies carried out for **46** and **47** (Fig. 19) corroborated the composition and ligand-bonding pattern established by NMR spectroscopy for diamagnetic Y and La species. In both complexes, the bond distances between the C_5-ring of the fluorenyl fragment in the chelating ligand and the metal center are consistent with an η^5-coordination mode (type **A**). A mechanical electron counting for these species would end-up to unrealistic value of 20. It turns out that the Cp ligand associated to the non-chelating fluorenyl moiety approaches the η^3-coordination (type **B**). Taking into account that the η^5-coordination of the coordinated fluorenyl unit is also unsymmetrical, **46** should be best described as an 18-electron complex. Effective direct *ansa*-chelation of $Me_2C(C_{13}H_9)(C_5H_5)$ onto lanthanides was achieved afterwards by using a salt metathesis route [42]. The reaction between $YCl_3(THF)_n$

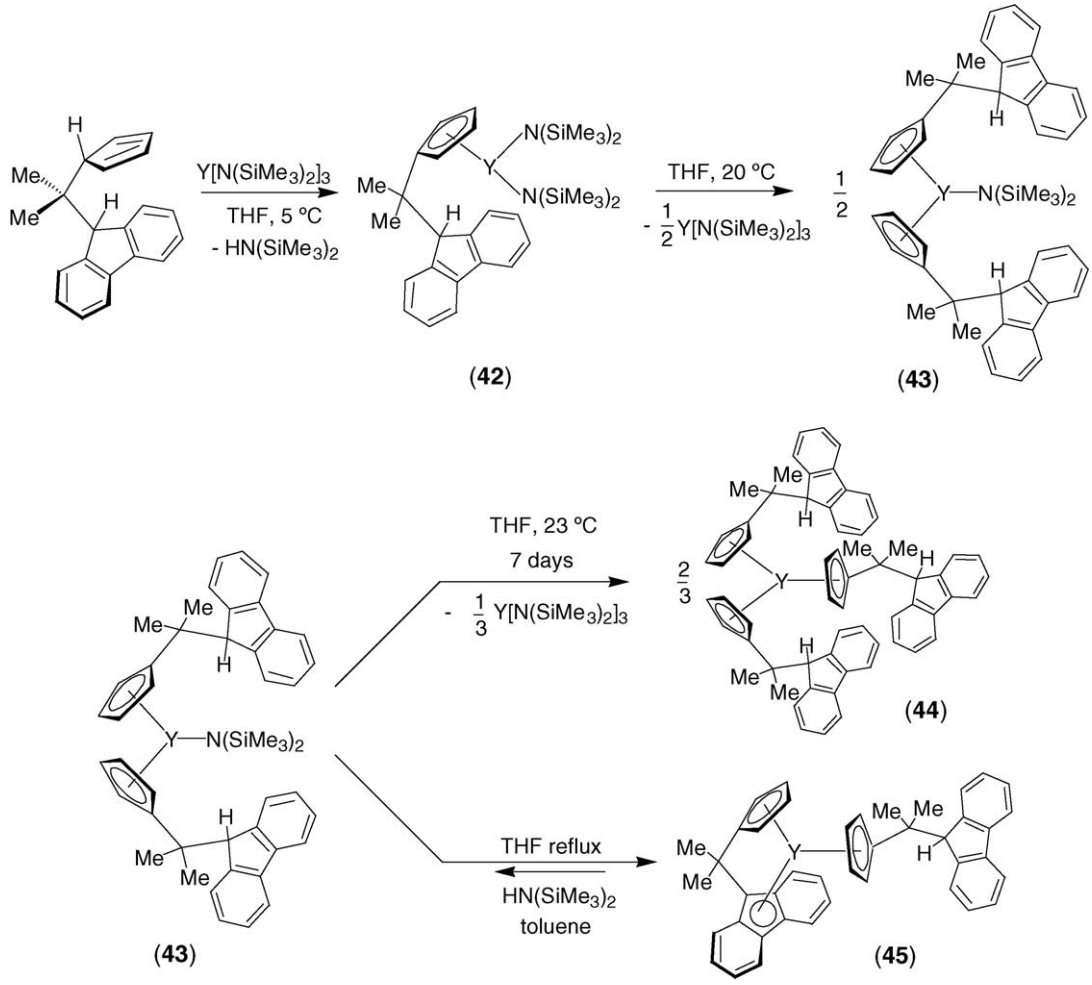

Scheme 13.

and 1 equiv. of the dilithium salt of this ligand in Et_2O solution unexpectedly led to the isolation of the bis(ligand) chlorine-free *ansa*-metallocene **49**, the first example of a bis-*ansa*-metallocene. The reaction proceeds first through the dichloro *ate*-complex $[Me_2C(C_{13}H_8)(C_5H_4)YCl_2]^-[Li(ether)_4]^+$ (**48**), which further disproportionates to **49** and YCl_4^- during the recrystallization course (Scheme 14).

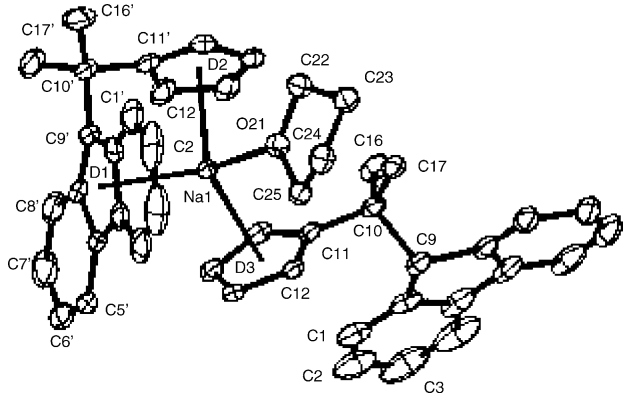

Fig. 19. The molecular structure of complex **47**. Reprinted with permission from Ref. [41]. Copyright 2002 American Chemical Society.

Interestingly, on using slightly different recrystallization protocols, three different crystal samples of the one and same compound **49**, i.e. monoclinic, triclinic and orthorhombic polymorphs, could be isolated and studied by X-ray analysis. Though the general atom connectivity of the three crystal structures is essentially the same (Fig. 20), noticeable differences in the geometric parameters and bonding features exist between these polymorphs, which arise from the large flexibility of this molecule. Complex **49** comprises a fully dissociated ion pair in the solid state with the cation composed by a lithium atom coordinated by four ether molecules. The yttrium atom in the anion is coordinated in a distorted tetrahedral geometry by two non-equivalent ligand units. An exocyclic η^3-bonding mode (type **F**) is found for one of the two fluorenyl moieties of the three polymorphs of **49**. The other fluorenyl moiety in the three polymorphs differs from the first one with an unprecedented η^1-bonding mode (type **G**) that involves merely one carbon (C(34)) of the benzene ring.

The bonding patterns of the fluorenyl ligands in **49** clarified from X-ray data were corroborated by a DFT study

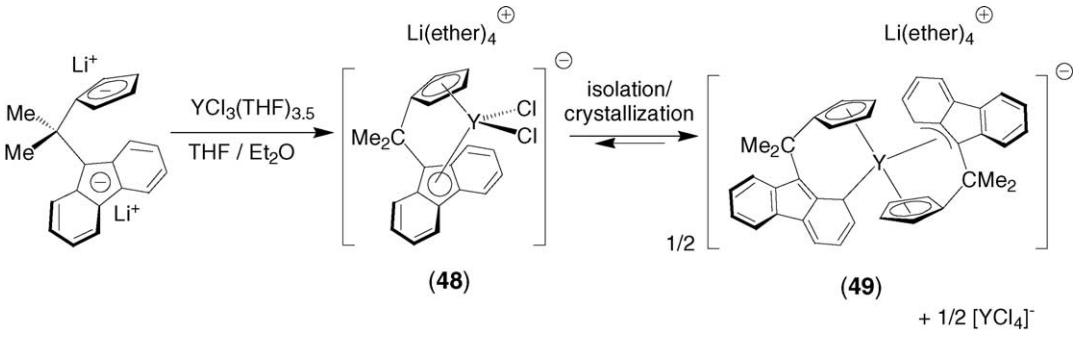

Scheme 14.

[42]. The Y–C Mulliken overlap populations determined by single-point calculations performed on the three experimental molecular structures are in agreement with the η^3-bonding mode of one fluorenyl moiety and η^1-bond of the second one with yttrium. This complicated coordination sphere around the metal atom allows it to satisfy the 18-electron rule.

Likewise, salt metathesis experiments conducted from $LaCl_3(THF)_n$ and 1 equiv. of $[Me_2C(C_{13}H_8)(C_5H_4)]Li_2$ led to the isolation of the parent ionic complex $[\{Me_2C(C_{13}H_8)(C_5H_4)\}_2La]^-[Li(Et_2O)_2]^+$ (**50**). The lanthanum analogue of **49** features a closely associated ion pair with a Cp-ring doubly coordinated to the lanthanum and lithium centers (Fig. 21). In contrast to **49**, both fluorenyl units in **50** are coordinated in an exocyclic η^3-mode (type **F**) that apparently arises from the large difference of ionic radii of yttrium and lanthanum.

The yttrium complex **49** in THF solution features a symmetric coordination of both $Me_2C(C_{13}H_8)(C_5H_4)$ moieties to the metal center on the NMR timescale. This observation suggests rapid exchange of bonding modes **G** and **F** between the two fluorenyl moieties and/or rapid symmetrization of bonding within each fluorenyl moiety via slippage from one

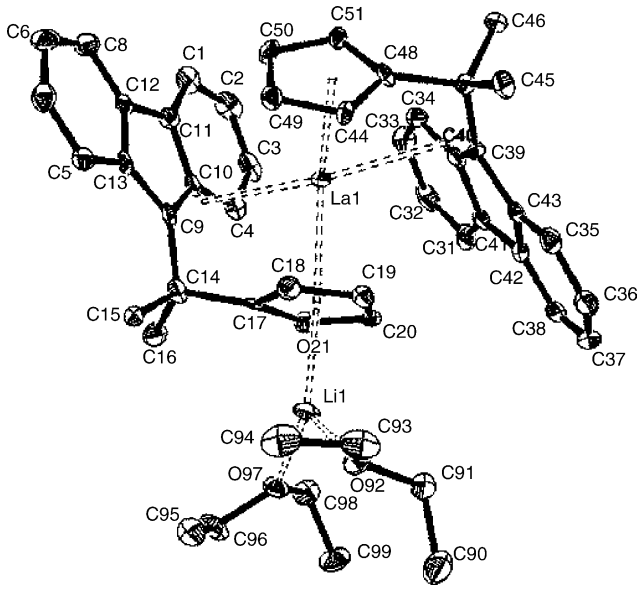

Fig. 21. The molecular structure of complex **50**. Reprinted with permission from Ref. [42]. Copyright 2003 American Chemical Society.

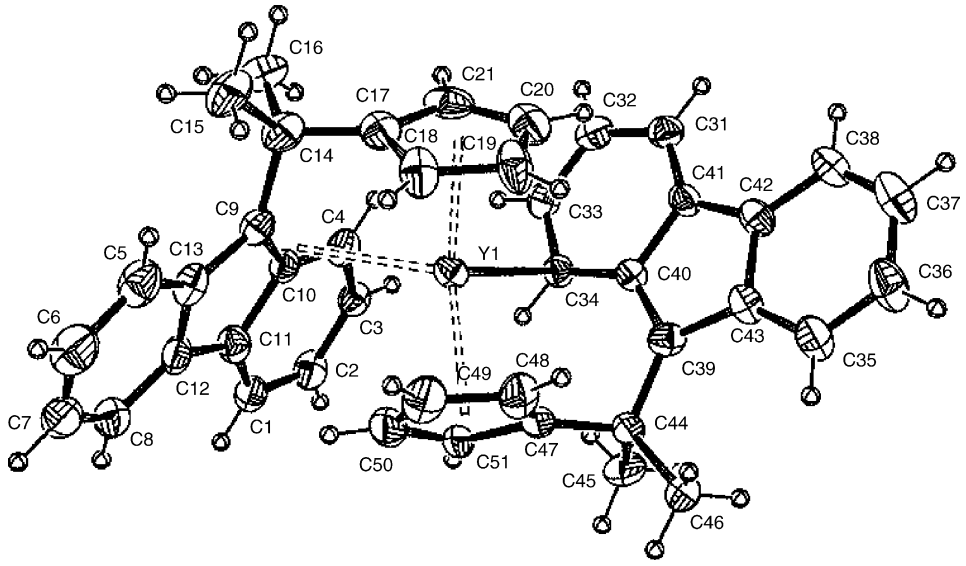

Fig. 20. The structure of the anion of one of the polymorphs of complex **49**. Reprinted with permission from Ref. [42]. Copyright 2003 American Chemical Society.

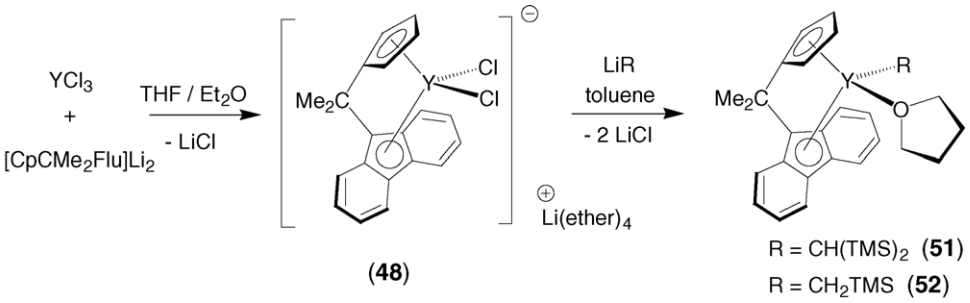

Scheme 15.

six-membered ring to the opposite side. The solution behavior of the lanthanum complex **50** revealed also a symmetric bis(*ansa*-metallocene) structure on the NMR time scale, consistent with dissociation of the ion pair. Not considering the Li cation, the solid-state molecular structure of **49** (Fig. 21) corresponds to a 20-electron species. It can be suggested, however, that the Cp ring, which coordinates both La and Li, donates only four electrons to La and behaves as a 2-electron donor to Li, via its totally in-phase π-bonding orbital. Within this hypothesis, the solid-state structure **50** would correspond to an 18-electron complex. It is possible that the dissociation of the ion pair in solution leads to partial decoordination of one of the fluorenyl moiety from η^3 (type **F**) to η^1 (type **D**) or η^2 in order to maintain the 18-electron count of the metal. As for **50**, rapid exchange of the bonding modes of the two fluorenyl ligands would render them symmetric on the NMR time scale.

The dichloro *ate*-complex **48** was successfully applied to the preparation of neutral yttrocene alkyl derivatives incorporating the $Me_2C(C_{13}H_8)(C_5H_4)$ ligand system [43]. It was shown that, despite the disproportionation via ligand redistribution observed upon crystallization of **48**, the latter reacts in solution as a single Y–Cl species (Scheme 15). Thus, alkyl complexes **51** and **52** were isolated in high yields and the identity of the former was confirmed by an X-ray diffraction study (Fig. 22).

The fluorenyl ligand in **51** was found to coordinate symmetrically to the yttrium center in an η^3-fashion (type **B**), indicative of a congested chelation. The constraint is also illustrated by the narrow bite angle Cp_{cent}–C–Flu_{cent} of 110.85°.

The most remarkable feature in the structure of **51** and **52** is the presence of a coordinated THF molecule despite the significant steric crowding of the metal center provided by the bulky fluorenyl/cyclopentadienyl and bis(trimethylsilyl) ligands. This coordinated THF molecule is labile in solution on the NMR time scale, leading to an equilibrium between a THF-free species and a THF adduct. Variable-temperature ^{1}H NMR allowed the measurement of the enthalpy and entropy of this dissociative process for both complexes (**51**: $\Delta_r H = 28 \pm 2$ kJ mol^{-1}, $\Delta_r S = 58 \pm 10$ kJ mol^{-1} K^{-1}; **52**: $\Delta_r H = 31 \pm 2$ kJ mol^{-1}, $\Delta_r S = 50 \pm 10$ kJ mol^{-1} K^{-1}).

Attempt to generate the corresponding benzyl complex by reacting **48** with $PhCH_2MgBr$ unexpectedly led to the isolation of $[(\eta^5,\eta^5\text{-}\{Me_2C(C_{13}H_8)(C_5H_4)\})Y(\mu\text{-Br})]_2$ (**53**) [43]. Complex **53** is only sparingly soluble in aromatic hydrocarbons and appeared to be unstable in THF hampering its authentication by NMR. However, its solid-state structure was determined and revealed a dimeric complex with bridging bromine atoms (Fig. 23). In this case, no coordinated THF molecule is present in the coordination sphere of yttrium and both fluorenyl fragments are unambiguously η^5-coordinated

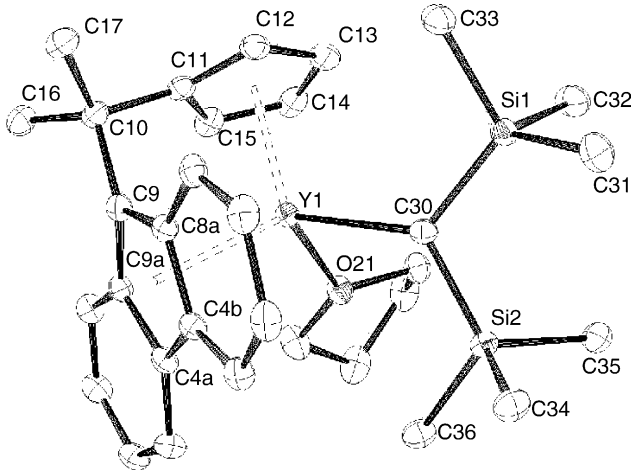

Fig. 22. The molecular structure of complex **51** [43].

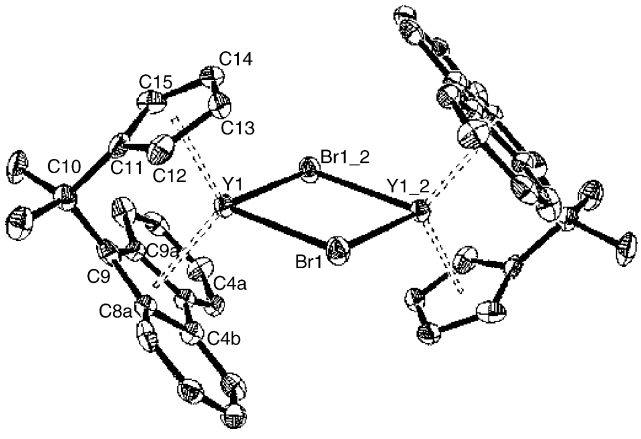

Fig. 23. The molecular structure of complex **53**. Reprinted with permission from Ref. [43]. Copyright 2004 American Chemical Society.

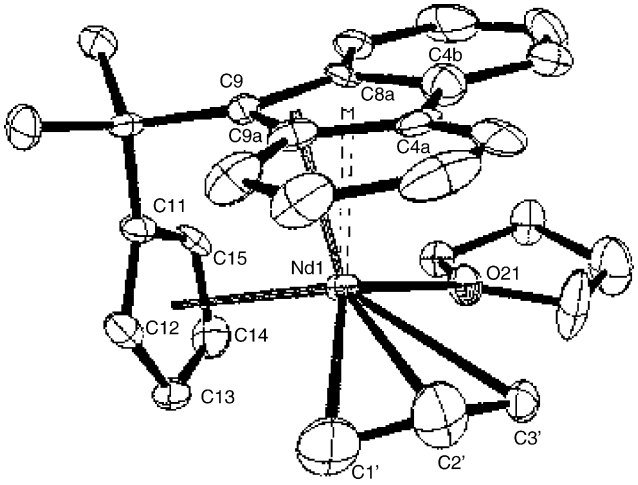

Fig. 24. The molecular structure of complex **56**. Reprinted with permission from Ref. [44]. Copyright 2004 American Chemical Society.

(type **A**), allowing the metals to achieve the stable 16-electron configuration in Cp_2ML_2 type of environment.

In striking contrast with the above-described reaction with benzylmagnesium bromide, the allyl Grignard reagent C_3H_5MgCl reacts with **48** in toluene solution to yield the desired allyl complex $\{Me_2C(C_{13}H_8)(C_5H_4)\}Y(C_3H_5)(THF)$ (**54**) [44]. The La (**55**), Nd (**56**) and Sm (**57**) homologues were prepared similarly in a "one-pot" procedure from the appropriate lanthanide trichloride and $Me_2C(C_{13}H_8)(C_5H_4)Li_2$ in Et_2O and subsequent reaction with C_3H_5MgCl in toluene solution. Diamagnetic complexes **54** and **55** were characterized by NMR spectroscopy and the solid-state structure of Nd complex **56** was determined by X-ray diffraction (Fig. 24). The crystal structure of **56** is reminiscent of the structures of the above-mentioned yttrium carbyls. The coordination of the fluorenyl unit is also best described as an η^3-mode (type **B**), although a (distorted) η^5 (type **A**) mode would describe **56** as an 18-electron complex. Complex **56** features a very narrow bite angle Cp_{cent}–C–Flu_{cent} of 93.88°, the smallest as ever seen in *ansa*-lanthanidocenes to our knowledge. The allyl fragment is η^3-bonded with the three carbon atoms displaying nearly equal participation.

Hydrogenolysis of the lanthanide alkyls constitutes a convenient synthetic approach toward hydrido derivatives, which are another important class of complexes. The first crystallographically characterized example of such derivative incorporating a fluorenyl-based ligand, i.e. $[(\eta^5,\eta^5\text{-}\{Me_2C(C_{13}H_8)(C_5H_4)\})Y(\mu\text{-}H)(THF)]_2$, was prepared by the reaction of either **51** or **52** with standard hydrogenolysis agents (H_2, $PhSiH_3$) in benzene solution [43]. Alternatively, the reduction of the chloro complex **48** with $NaBHEt_3$ in toluene solution provides a more direct route to **57**. Complex **57** features a dimeric solid-state molecular structure with bridging hydride and "spanned" $Me_2C(C_{13}H_8)(C_5H_4)$ ligands (Fig. 25). The Y–H bond lengths were found to be short, 1.99(4) and 2.01(4) Å, and both fluorenyl moieties are clearly η^5-bonded to yttrium (type **A**).

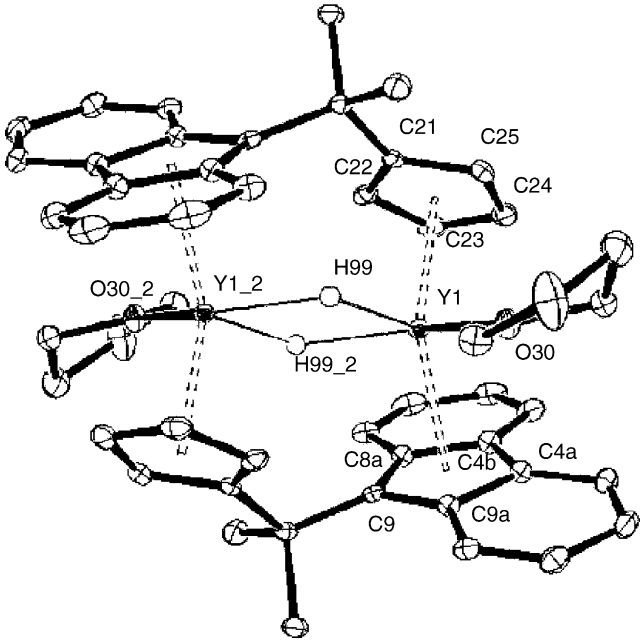

Fig. 25. The molecular structure of complex **57**. Reprinted with permission from Ref. [43]. Copyright 2004 American Chemical Society.

The influence of bulky substituents on the coordination sphere of the metal center was investigated with the modified ligand system $[(3\text{-}^t\text{Bu–}C_5H_3)\text{–}CMe_2\text{–Flu}]^{2-}$ (Scheme 16) [43]. The salt elimination reaction of the dilithium salt of this ligand with $YCl_3(THF)_{3.5}$ gave $[(3\text{-}^t\text{Bu–}C_5H_3)\text{–}CMe_2\text{–Flu}]YCl(THF)$ (**58**), which was subsequently treated with 1 equiv. of $LiCH(SiMe_3)_2$ to afford the THF-free alkyl complex **59** in high yield. The consistency of both yttrocenes was confirmed by NMR spectroscopy.

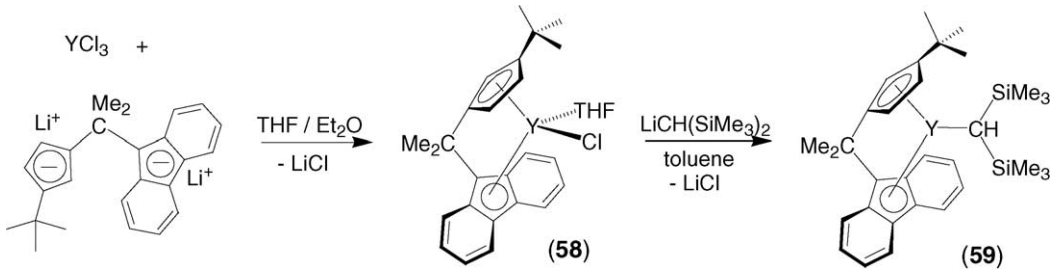

Scheme 16.

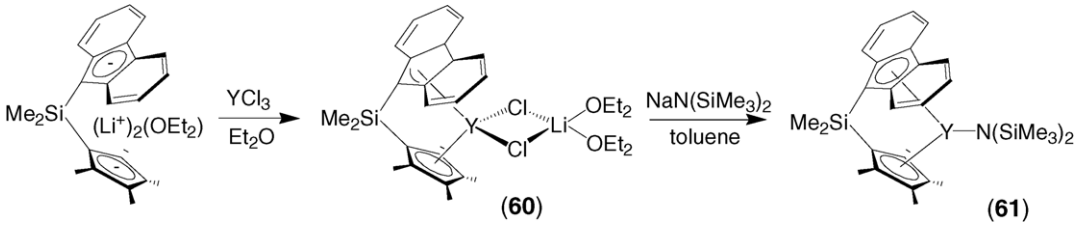

Scheme 17.

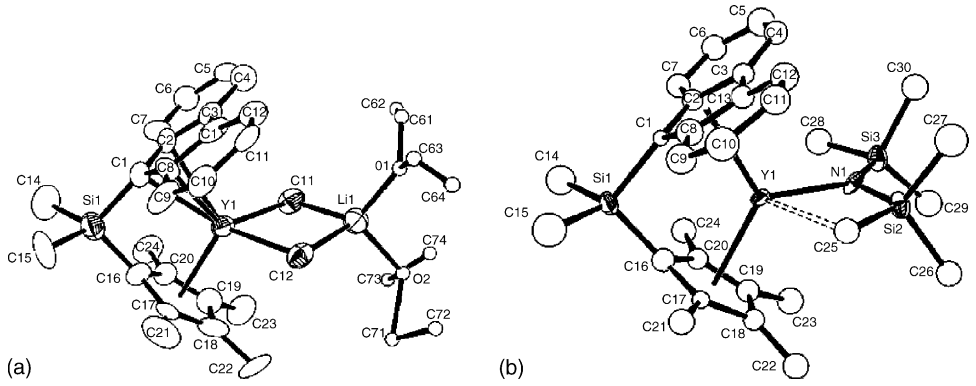

Fig. 26. The molecular structures of complexes **60** (a) and **61** (b). Reprinted with permission from Ref. [45]. Copyright 1999 American Chemical Society.

4.3. ansa-Metallocenes bearing silylene-bridged fluorenyl-based ligands

This class of fluorenyl complexes of lanthanides is thus far limited to a few examples described in the works of Qian and Do.

The bulky silylene-bridged fluorenyl-tetramethylcyclopentadienyl ligand was used by Do and co-workers to prepare the *ansa*-yttrocenes $\{Me_2Si(C_{13}H_9)(C_5Me_4)\}YCl_2Li(Et_2O)_2$ (**60**) and $\{Me_2Si(C_{13}H_9)(C_5Me_4)\}Y[N(SiMe_3)_2]$ (**61**) (Scheme 17) [45].

Complex **60** constitutes a rare example of a "classic" *ate* complex bearing a fluorenyl ligand in which both the yttrium and lithium centers are linked to the bridging Cl atoms (Fig. 26a). The large steric crowding in the coordination sphere of these *ansa*-lanthanidocenes can be evaluated from the bite angle values, which are normally 10–15° larger for silylene-bridged metallocenes than those for carbon-bridged systems. The bite angles Cp_{cent}–C–Flu_{cent} in **60** and **61** are 125.3° and 123.7°, respectively. An endocyclic η^3-coordination (type **B**) of the fluorenyl moiety with yttrium was clearly concluded in complex **60**, whereas in complex **61** the coordination is intermediate between the η^3 and η^5 modes (Fig. 26b). X-ray diffraction data also revealed a strong agostic interaction between a carbon atom from the bis(trimethylsilyl)amido group and the metal center in **61**.

A series of silylene-bridged *ansa*-metallocenes of yttrium, lutetium, dysprosium and erbium incorporating fluorenyl/cyclopentadienyl ligands were synthesized by Qian et al. using a salt metathesis approach (Scheme 18) [46,47]. In contrast to the fluorenyl-tetramethylcyclopentadienyl yttrocene **60**, neutral dimeric complexes are formed in this case, i.e. $[\{R_2Si(C_{13}H_8)(R'C_5H_3)\}LnCl]_2$ (R = Me, R′ = H, Ln = Y, **62**; Lu, **63**; Dy, **64**; Er, **65**; R = Ph; R′ = ^{t}Bu, Ln = Y, **66**; Dy, **67**).

The crystal structures of two of them (**62** and **66)** were determined by X-ray analysis and shown to feature a "spanned" coordination of the fluorenyl/cyclopentadienyl

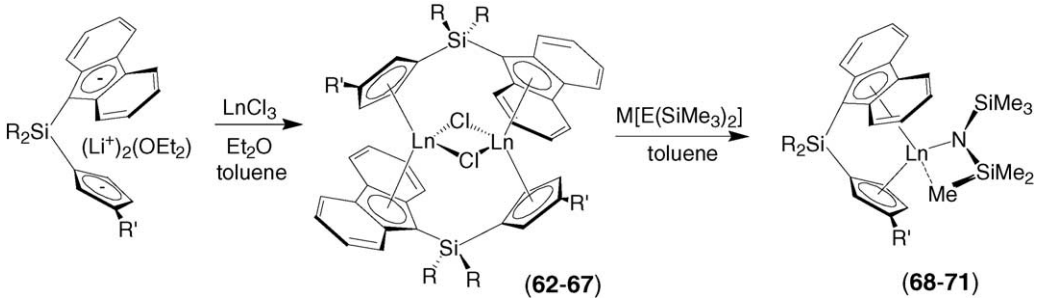

Scheme 18.

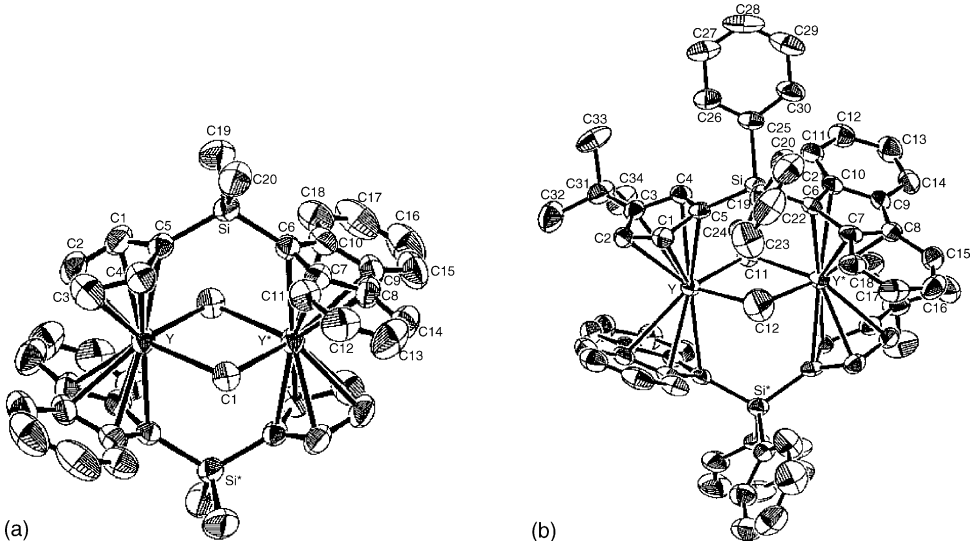

Fig. 27. The molecular structures of complexes **62** (a) and **66** (b). Reprinted with permission from Refs. [46,47]. Copyright 2000 American Chemical Society and 2002 Elsevier.

ligands, independent on the nature and bulkiness of the substituents on the bridge and Cp ring (Fig. 27a and b). However, the bonding modes of the fluorenyl units in **62** and **66** are not exactly the same, that is an η^5 coordination (type **A**) and a slipped mode toward η^3 (type **B**), respectively.

Treatment of these chloro complexes with $LiCH(SiMe_3)_2$ and $KN(SiMe_3)_2$ resulted in the formation of the alkyl and amido derivatives $\{Me_2Si(C_{13}H_8)(C_5H_4)\}Ln[E(SiMe_3)_2]$ (E = N, Ln = Dy, **68**; Er, **69**; E = CH, Ln = Dy, **70**; Er, **71**) (Scheme 18). This reaction is accompanied by the rearrangement of the "spanned" ligand into an *ansa*-chelating pattern, as confirmed by the X-ray diffraction studies performed on **68** and **70** (Fig. 28). Both these complexes show close structural similarities; in particular, the bonding features of the fluorenyl moieties with metals are nearly the same, i.e. slipped to η^3 from η^5 (type **B**). However, the amido complex **68** features an agostic interaction of a trimethylsilyl carbon atom with dysprosium, while no interaction was found in **70**.

Also, a "neutral" silylene-bridged bis(fluorenyl) neodymocene, tentatively formulated $Me_2Si(C_{13}H_8)_2NdCl$ (**72**), was prepared by the reaction of $Me_2Si(C_{13}H_8)_2Li_2$ salt with $NdCl_3$ in THF [48]. No exhaustive characterization was provided for this complex that has been used as a polymerization catalyst precursor (vide infra).

The "extended" amine elimination reaction of homoleptic yttrium amide $Y[N(SiHMe_2)_2]_3(THF)_n$ with *diproteo* Me_2Si(cyclopentadienyl–H)$_2$ was investigated in detail by Anwander and co-workers [49]. However, partly because of the low acidity of fluorenyl protons in $Me_2Si(C_{13}H_9)_2$, this reaction appeared to be disfavored and gave a poor yield (<7%) of the *ansa*-metallocene product $\{Me_2Si(C_{13}H_8)_2\}Ln[N(SiHMe_2)_2]$ (**73**).

4.4. Constrained-geometry fluorenyl-based systems

The σ-bond metathesis approach was intensively investigated as a convenient entry toward half-sandwich lanthanide complexes incorporating constrained-geometry fluorenyl-based ligands [50]. The amine elimination reaction between homoleptic lanthanide amides $Ln[N(SiMe_3)_2]_3$ and

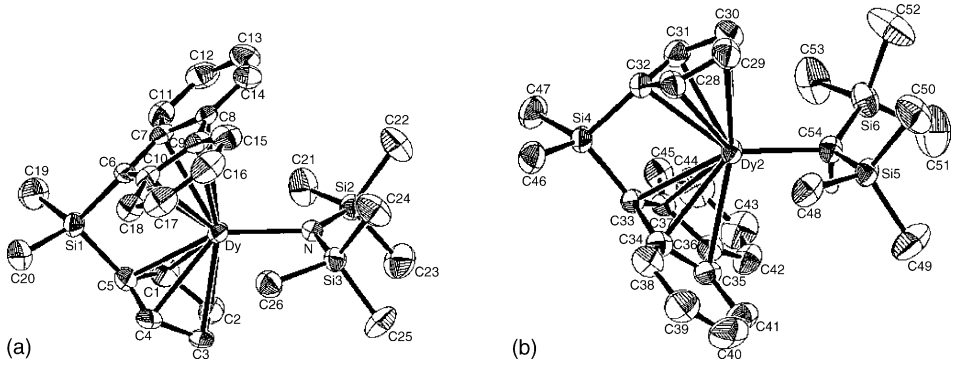

Fig. 28. The molecular structures of complexes **68** (a) and **70** (b). Reprinted with permission from Refs. [46,47]. Copyright 2000 American Chemical Society and 2002 Elsevier.

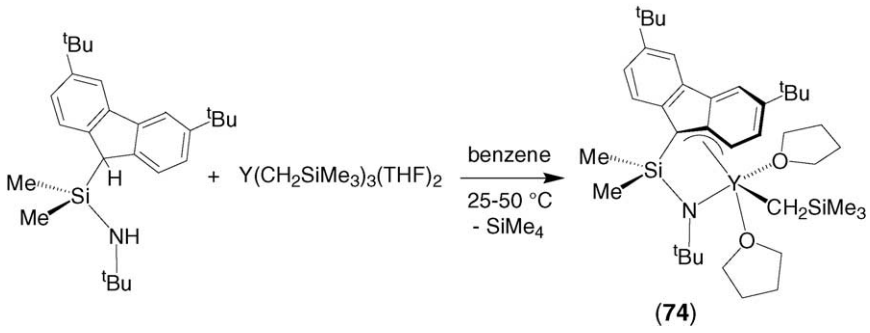

Scheme 19.

diproteo $R_2Si(3,6\text{-}^tBu_2C_{13}H_7)(NH^tBu)$ (R = Me, Ph) ligands was found inoperative, again most likely due to the low acidity and, consequently, poor reactivity of both fluorenyl and amido groups. In remarkable contrast to amine elimination, alkane elimination from yttrium trialkyl $Y(CH_2SiMe_3)_3(THF)_2$ proved to be a much more efficient route (Scheme 19). Quantitative conversion of the *diproteo* ligand $Me_2Si(3,6\text{-}^tBu_2C_{13}H_7)(NH^tBu)$ into the half-sandwich complex **74** was readily achieved, whereas the more bulky ligand $Ph_2Si(3,6\text{-}^tBu_2C_{13}H_7)(NH^tBu)$ appeared less reactive toward $Y(CH_2SiMe_3)_3(THF)_2$ (and the final product more thermally sensitive), resulting in low yields.

The crystal structure of **74** revealed that, in the solid state, the fluorenyl moiety is bonded with yttrium in an unusual exocyclic η^3-fashion (type **F**) (Fig. 29). The presence of an additional THF molecule in **74**, as compared to "constrained-geometry" cyclopentadienyl-based yttrium analogues that contain only one coordinated-THF molecule, constitutes a specific feature of this 12-electron complex that may be directly connected to the reduced hapticity of the fluorenyl ligand. Interestingly, the reduced η^3 hapticity of the fluorenyl unit seems to be preserved in solution, as judged by variable-temperature NMR spectroscopy. One of the two coordinated THF molecules is labile on the NMR time scale and involved into a dissociative process between the mono- and di-solvated forms of complex **74**.

Generation of the related hydrido derivative from the yttrium carbyl **74** by reaction of the latter with H_2 or $PhSiH_3$ gave a yellow product (**75**) that is insoluble in common organic solvents (aromatic hydrocarbons, chlorinated solvents, THF), despite the presence of two *tert*-butyl substituents (Scheme 20). The reaction of this putative hydride with an excess of pyridine at 70 °C resulted in the new pyridine-insertion "constrained-geometry" yttrium amido complex **76**, the identity of which was established by NMR spectroscopy and X-ray analysis (Fig. 30) [51]. Complex **76** displays a pseudo-five-coordinate geometry that is very similar to its alkyl parent **74**, with the THF molecules and the alkyl group in **74** being replaced by pyridine molecules and a dihydropy-

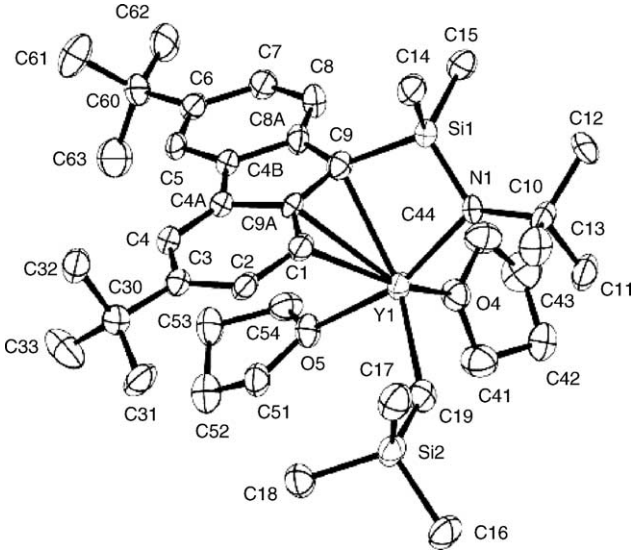

Fig. 29. The molecular structure of complex **74**. Reprinted with permission from Ref. [50]. Copyright 2003 American Chemical Society.

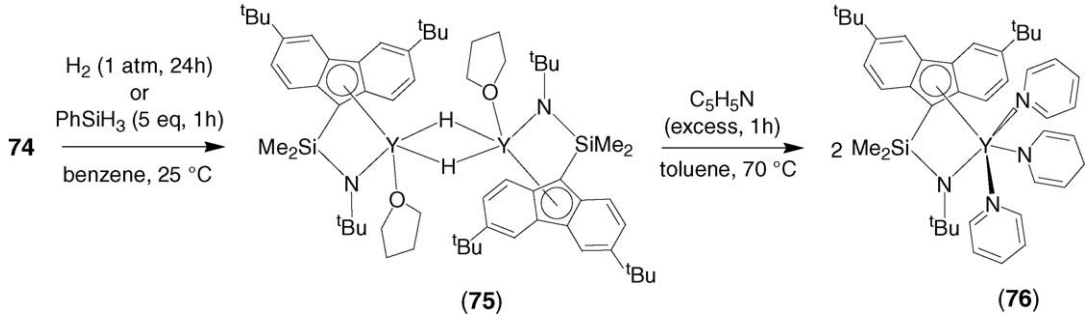

Scheme 20.

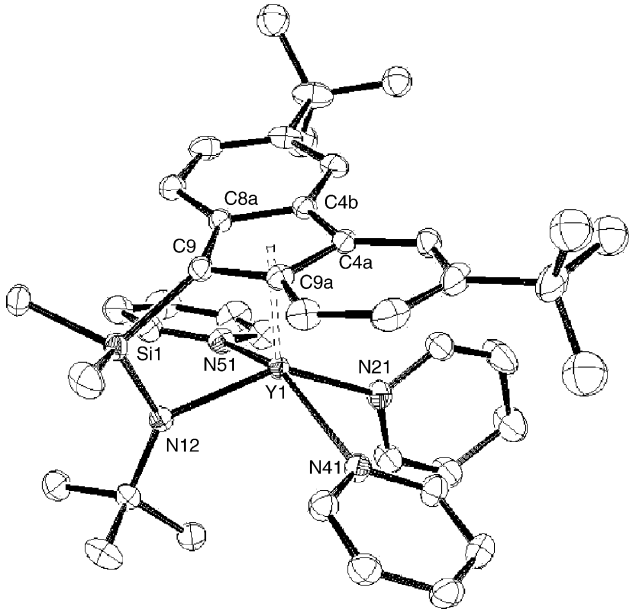

Fig. 30. The molecular structure of complex **76**. Reprinted with permission from Ref. [51]. Copyright 2004 Wiley.

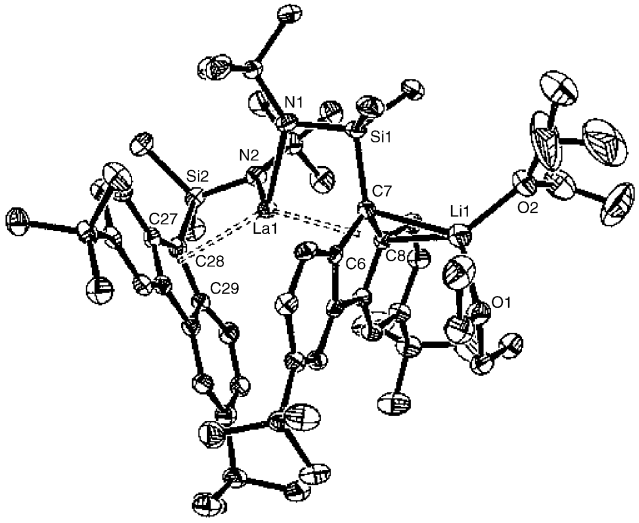

Fig. 31. The molecular structure of complex **78**. Reprinted with permission from Ref. [50]. Copyright 2003 American Chemical Society.

ridinyl group in **76**, respectively. However, in contrast with the unusual non-symmetric, exocyclic η^3 coordination mode of the fluorenyl moiety observed in the solid-state structure of **74**, that of **76** features a symmetric η^5 coordination (type **A**) resulting in a higher electron count (14-e).

Salt elimination reactions between the dilithium salt $Me_2Si(3,6\text{-}^tBu_2C_{13}H_6)(N^tBu)Li_2$ and lanthanide trichloride precursors were explored and resulted in most cases in the formation of the anionic bis(ligand) disproportionation products of general formula $[\{Me_2Si(3,6\text{-}^tBu_2C_{13}H_6)(N^tBu)\}_2Ln]^-[Li(ether)_n]^+$ (Ln = Y, ether = THF, $n = 4$, **77**; Ln = La, ether = Et_2O, $n = 2$, **78**) [50]. These diamagnetic complexes were isolated in good yields and authenticated by NMR spectroscopy and an X-ray diffraction study for **78** (Fig. 31). The solid-state structure of **78** features a closely associated ion pair. Each of the fluorenyl moieties is coordinated in an η^3-fashion involving the bridgehead carbon atom of the central five-membered ring and the two adjacent carbon atoms fusing the five- and six-membered rings. Such allylic coordination of the two fluorenyl units is, however, not as symmetric as in the ideal case **B** and the lanthanum atom is, therefore, slipped on one side of the fluorenyl system. A limit view of an η^2 coordination mode for both fluorenyl units would render **78** isostructural and isoelectronic to tetrahedral ML_4 8-electron complexes.

When the same salt metathesis synthetic approach was applied to neodymium chemistry, the disproportionation product $[\eta^3,\eta^1\text{-}\{(3,6\text{-}^tBu_2C_{13}H_6)SiMe_2N^tBu\}_2Nd(THF)]^-[Li(THF)_4]^+$ (**79**) was isolated in poor yield (Scheme 21) [50]. Crystallization of the crude product from Et_2O:hexane solution allowed the isolation of the neutral chloro complex $[\eta^5,\eta^1\text{-}\{(3,6\text{-}^tBu_2C_{13}H_6)SiMe_2N^tBu\}Nd(\mu\text{-}Cl)(THF)]_2$ (**80**), which is the major product formed in this process. The identity of both complexes was unambiguously established by single-crystal X-ray diffraction studies (Fig. 32a and b).

The molecular structure of **79** in the solid state comprises a fully dissociated ion pair in which the cation consists of a lithium atom coordinated by four THF molecules. The neodymium atom is coordinated in a distorted trigonal bipyramidal geometry by one THF molecule and a pair of amido and fluorenyl moieties. In contrast with the parent anionic bis(ligand) lanthanum complex **78**, but similarly to neutral yttrium carbyl **74**, both fluorenyl moieties in **79** are coordinated to Nd in a dissymmetric fashion. A clear dissymmetric η^3-bonding mode (type **F**) is established for one fluorenyl ligand. The corresponding Nd–C(Flu) bond distances for the second ligand indicates that this fluorenyl ring may be in a stage of approaching towards reduced hapticity (η^2 or η^1 bonding mode, type **G**).

4.5. Miscellaneous reactions

Introduction of fluorenyl fragments in the coordination environment of samarium metal by reduction of *N*-phenyl-fluorenimine with divalent samarium precursors $Sm(OAr)_2(THF)_3$ and $Sm[N(SiMe_3)_2]_2(THF)_2$ was demonstrated by Hou et al. (Scheme 22) [52]. The crystal structures of the recovered products **81** and **82** appeared to be very similar, featuring identical bonding fashions of the fluorenyl moieties with samarium via the bridgehead atom (type **D**) (Fig. 33a and b).

5. Applications in catalysis

Applications in catalysis of fluorenyl complexes of groups 2 and 3 metals are promising since, in principle, they could

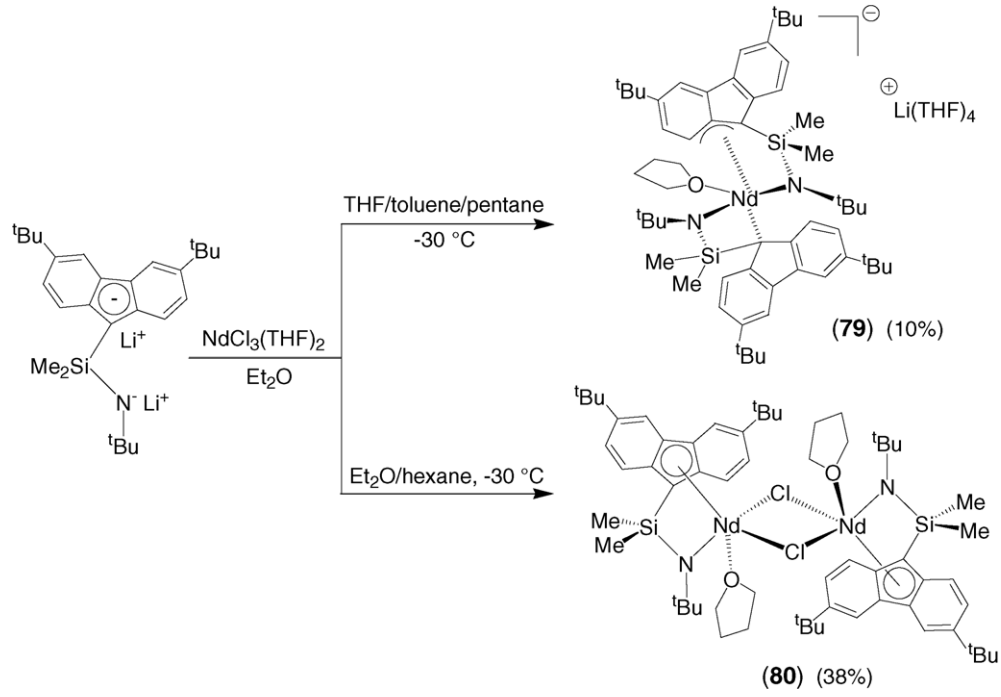

Scheme 21.

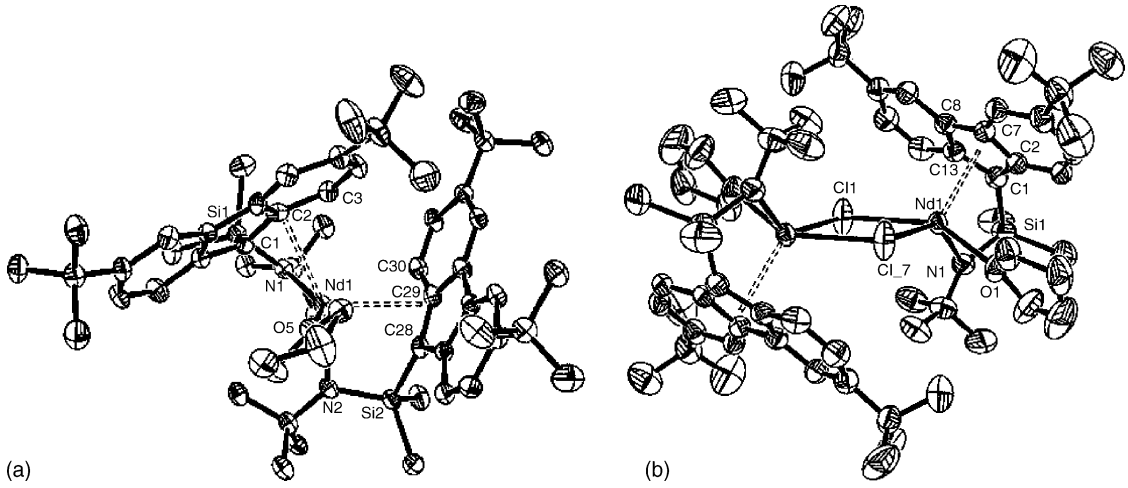

Fig. 32. The molecular structures of complexes **79** (a) and **80** (b). Reprinted with permission from Ref. [50]. Copyright 2003 American Chemical Society.

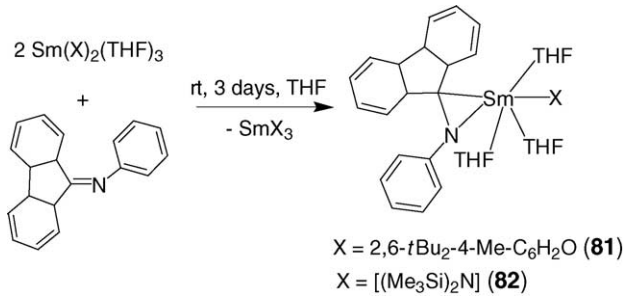

Scheme 22.

cover the same areas as those efficiently performed by a plethora of cyclopentadienyl group 3 metal complexes, in particular polymerization of polar and non-polar monomers [53], and a variety of C–C and C–X (X = H, B, N, Si, P) bond-forming reactions [54]. They could also take advantage of the unique features brought by the fluorenyl moiety in group 4 metallocene chemistry [2]. Recent years have indeed witnessed a growing interest in the investigation of the catalytic performances of these groups 2 and 3 metal fluorenyl complexes, although only a restricted numbers of convincing examples have been disclosed thus far.

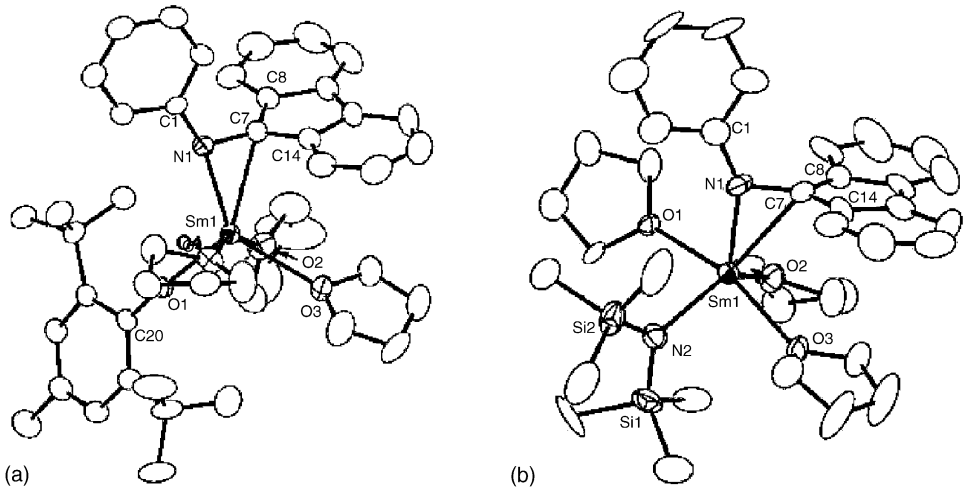

Fig. 33. The molecular structures of complexes **81** (a) and **82** (b). Reprinted with permission from Ref. [52]. Copyright 2003 American Chemical Society.

5.1. Polymerization of polar monomers

The divalent bis(fluorenyl)samarocene **3** was shown by Evans and Katsumata to be active in the ring-opening copolymerization of ethylene carbonate (EC) and ε-caprolactone (ε-CL) at room temperature [55]. The copolymer, obtained in 63% yield, contained ca. 14 mol% of ε-CL and had a number-average molecular weight M_n of 28,000 and a rather large polydispersity M_w/M_n of 2.3. Monometallic **10** and heterotrimetallic **12** samarocenes displayed no activity towards methyl methacrylate (MMA) but were highly active in the ring-opening polymerization of ε-CL, providing at full conversion PCL polymers with low molecular weight (M_n = 5500–7300) and very narrow polydispersity (M_w/M_n = 1.17–1.20) [19]. The divalent ytterbium complex **15** and its dinuclear derivative **16** initiate the polymerization of MMA at −40 °C giving isotactic-enriched PMMA (*mm* triads ≈ 80%) with M_n = 127,000–244,000 and M_w/M_n = 1.62–2.08 [21,22]. The activity of **16** was found to be ca. 5 times higher than that of **15** and amounts to $1.4 \times 10^{-5}\%_{conversion}\ mol^{-1}\ min^{-1}$.

The trivalent carbon-bridged *ansa*-metallocene amide **41** was found to be only slightly active in the polymerization of MMA giving syndiotactic-enriched polymer (*rr* triads 59%) with M_n = 24,000 and M_w/M_n = 2.27 [40]. A somewhat higher activity was noted towards ε-CL and δ-valerolactone, cyclic monomers which are traditionally more reactive. In comparison, the yttrium hydrocarbyls **51** and **52** were found to be much more active in the polymerization of MMA under mild conditions (−15 to 20 °C), yielding syndiotactic-enriched PMMA (*rr* 60–66%) with high molecular weight (M_n = 271,000–376,000) and M_w/M_n = 1.43–1.87 [43]. Comparable and even higher activity for MMA polymerization was provided by silicon-bridged *ansa*-metallocenes of trivalent lanthanides. For example, complex **61** gave syndiotactic-enriched PMMA (*rr* 56–58%) with M_n = ca. 110,000 and M_w/M_n = 1.29–1.39 [45]. Also, complexes **68**–**71** initiate MMA polymerization from −78 to 20 °C to yield syndiotactic-enriched polymers with very high molecular weights that are insoluble in THF [46].

The "constrained-geometry" yttrium alkyl **74** and "hydride" **75** complexes were found almost inactive towards MMA, whereas the anionic complex of lanthanum **78** smoothly reacts with MMA in the temperature range 20–50 °C to give atactic PMMA with high molecular weight (M_w = 216,000–250,000) and M_w/M_n = 2.8–3.6 [50].

5.2. Polymerization of styrene

The divalent complexes of ytterbium **4** and samarium **10** and **12** polymerize styrene (St) only sluggishly under ambient conditions [56]. In contrast, effective controlled syndiotactic polymerization of St was achieved by Harder et al. by using benzylic-fluorenyl complexes of alkaline-earth metals [32,34]. The polymerization proceeded in bulk St in the temperature range −20 to 20 °C in the presence of benzyl calcium complexes **30**–**32** and gave PSt with M_n = 96,000–109,000 and M_w/M_n = 2.04–2.35. The significant syndiotacticity (*rr* = 83–86%) of the PSt samples was illustrated by the $^{13}C\{^1H\}$ NMR spectrum of the aromatic region (Fig. 34) [57]. The benzyl-ytterbium analogue **33** featured similar high activity (100% conversion) giving PSt with M_n = 201,000 and M_w/M_n = 2.30, but lower syndiotacticity (*rr* ca. 67%) [24].

Upon exploring the catalytic activity of the carbon-bridged *ansa*-allyl-lanthanide complexes **54**–**57**, highly syndiospecific polymerization of styrene was achieved [44]. Polymerization of bulk St led to 70–85% maximum monomer conversions, while introduction of toluene in polymerization media was found detrimental for catalyst activity. The polymerization activity of the allyl complexes was in the order Nd (**56**) > Sm (**57**) > La (**55**) > Y (**54**), featuring a remarkably high activity of 250–1710 kg PS $mol^{-1}\ h^{-1}$ for complex **56**. The molecular weights were in the range

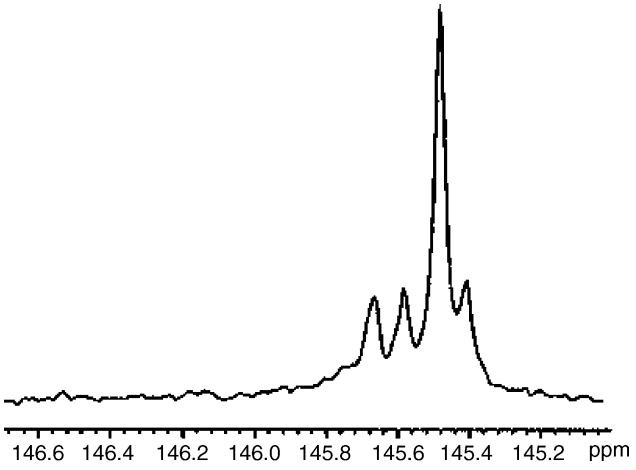

Fig. 34. The $^{13}C\{^1H\}$ signal of the phenyl C_{ipso} in the syndiotactic-enriched polystyrenes obtained from complexes **30**–**32**.

M_n = 10,000–135,000 with narrow to usual molecular weight distributions M_w/M_n of 1.25–2.10. The very high syndiotacticity (*rrrr* pentads > 99%) of the PSt samples obtained was illustrated by $^{13}C\{^1H\}$ NMR spectroscopy (Fig. 35) and other techniques.

5.3. Polymerization of ethylene

The potential of fluorenyl-lanthanide complexes to catalyze ethylene polymerization was investigated as well, but rather modest performances have been reached thus far. Both monometallic and trimetallic samarocenes **10** and **12** produce polyethylene (PE) (activity 0.03–1.72 kg PE mol^{-1} h^{-1} atm^{-1} at 25–65 °C and 1 atm of C_2H_4) with low molecular weight (M_n = 26,000–53,000) and monomodal, though rather broad polydispersity of 1.98–2.56 [19]. Only traces of PE were obtained using the THF-free bromo complex **53** activated with $[HAl(^iBu)_2(n\text{-}Bu)]^-Li^+$ ($HAl(^iBu)_2$/*n*-BuLi/Y = 40:40:1; cyclohexane, 80 °C, 8 atm) [43]. Applying the same activator and polymerization conditions with the *tert*-butyl-substituted mono-THF precursor **58** gave a moderately active catalyst (76 kg mol^{-1} h^{-1}), offering quite low-molecular-weight polyethylene (M_n = 900, M_w/M_n = 2.02, T_m = 124 °C) [43].

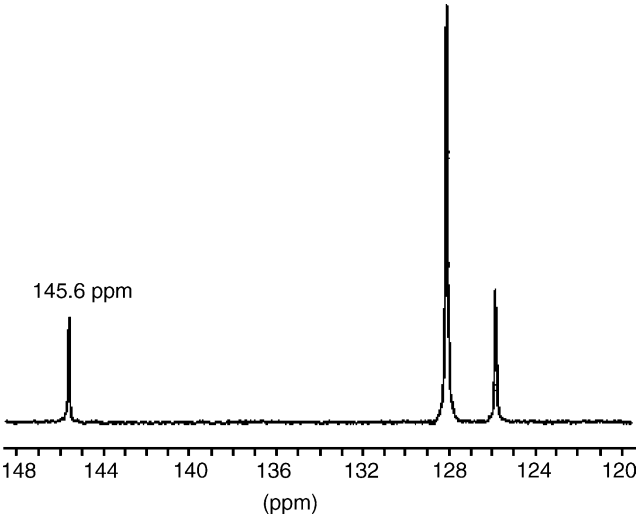

Fig. 35. Aromatic region of the $^{13}C\{^1H\}$ NMR spectrum of highly syndiotactic PSt obtained from complexes **54**–**57**.

Interestingly, the "constrained-geometry" yttrium hydrocarbyl **74** was found to be inactive towards ethylene [50], in contrast to its cyclopentadienyl equivalent [58]. The inactivity of the former most likely stems from the presence of two THF molecules in the coordination sphere of yttrium that might block the "active-site"; indeed, the cyclopentadienyl equivalent contains only one THF molecule, which was shown to decoordinate rather fast in solution [58]. The neutral dimeric neodymium chloride **80**, when activated with 1 equiv of $LiCH(SiMe_3)_2$, polymerizes ethylene with low activity (1.3 kg PE mol^{-1} h^{-1} atm^{-1} at 20 °C and 4 atm of C_2H_4) to yield PE with T_m = 134 °C, M_n = 140,000 and M_w/M_n = 2.46 [50]. Also, only traces of PE were obtained on using in situ combinations **80**/$Mg(^{n,s}Bu)_2$ (1:40) or **10**/$HAl(^iBu)_2/^nBuLi$ (1:20:20) as catalyst system under similar conditions.

5.4. Copolymerization of dienes and ethylene

An interesting and specific application of fluorenyl-lanthanide complexes in catalysis consists of the copolymerization of dienes with ethylene and/or α-olefins, which is a quite demanding process. Recently, Boisson et al. have shown that the *ansa*-neodymocene **72** upon activation with alkylating agents, e.g. $[HAl(^iBu)_2(^nBu)]^-Li^+$ or $Mg(alkyl)_2$, enables the copolymerization of ethylene with butadiene at 80 °C and 4 bar to give polymers with low to high molecular weight (M_n = 8000–148,000) and controlled polydispersity (M_w/M_n = 1.2–3.1) [59]. The copolymers featured unusual microstructures with high content (53–57%) of 1,2-cyclohexane rings. The latter could be rationally explained on the basis of a 2,1-insertion of butadiene, followed by two successive ethylene insertions and a final intramolecular insertion of a pending vinyl unit from butadiene (Scheme 23).

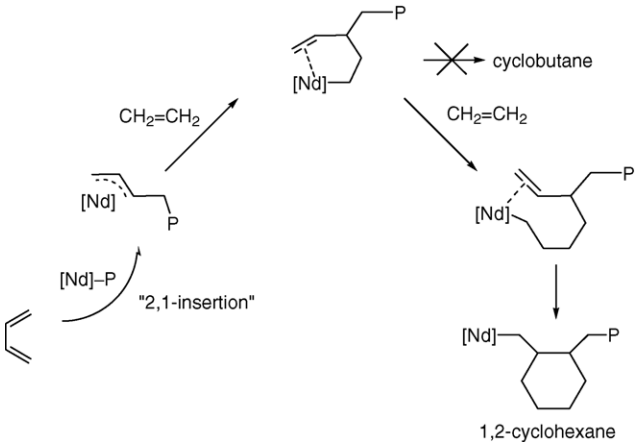

Scheme 23.

5.5. Comparison of polymerization catalytic performances of groups 2 and 3 fluorenyl complexes with related catalyst systems

Considering the aforementioned synthetic difficulties inherent to groups 2 and 3 metal chemistry and also to the fluorenyl ligands (as compared to group 4 metal chemistry and more easily introduced simple Cp ligands), it is worth questioning about the added value that those systems could bring to polymerization catalysis. The examples depicted in Sections 5.1–5.4 clearly demonstrate a contrasting situation.

The poor activities observed in the polymerization of ethylene and above all of higher α-olefins are in striking contrast with the outstanding abilities of fluorenyl-based group 4 metallocenes and hemi-metallocenes (constrained-geometry catalysts), which have demonstrated, in addition to high activity, very high efficiency in controlling the stereospecificity and livingness of the polymerizations of these monomers [2]. If this situation is not surprising for the polymerization of α-olefins, which has remained since the 1980s probably the major limitation for lanthanides [53a,b], the generally modest ethylene polymerization performances were less expected. Also, even if interesting results have been obtained in the polymerization of polar monomers such as MMA or caprolactone, fluorenyl complexes of alkaline earth and rare-earth metals do not challenge simpler lanthanidocenes or in situ binary combinations of lanthanide salts and alkylating agents [53c].

Much more significant are the recent advances obtained in the homopolymerization of styrene and the copolymerization of dienes with ethylene or α-olefins. Clearly, fluorenyl complexes of alkaline earth and lanthanides have offered activities and tacticities for styrene polymerization that have no precedent thus far with group 4 metallocenes. In this regard, one may argue that the dramatic improvement of activity for styrene polymerization may originate in the higher ionic character of groups 2 and 3 metal complexes as compared to that of analogous group 4 complexes. Even more promising is the unique ability of some fluorenyl-neodymium systems to achieve effective copolymerization of butadiene with ethylene and even α-olefins and afford original microstructures. Comparable investigations with group 4 metallocenes have thus far provided poor results, i.e., a large decrease in activity in the presence of conjugated dienes and low butadiene insertion [59].

5.6. Miscellaneous applications in catalysis for fine chemicals

The intramolecular hydroamination/cyclization of α,ω-aminoalkenes catalyzed by the constrained-geometry alkyl complex **74** was briefly investigated (Scheme 24) [60]. High selectivity but moderate activity was observed for this process, in contrast to highly active cyclopentadienyl-based lanthanidocenes [54b], most likely due to competitive coordination between molecules of THF in **74** and the amino substrate.

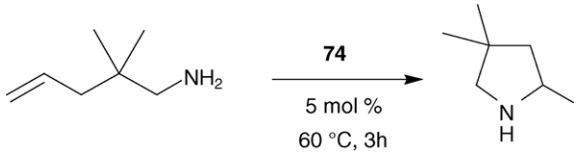

Scheme 24.

6. Conclusion

The fluorenyl ligand offers a surprisingly large variety of coordination modes (Scheme 2). Among them, those corresponding to type **A** (η^5) and type **B** (η^3) are by far the most common. The reasons for this preference are essentially electronic in origin. In particular, the bridgehead carbon is expected in general to bind to a metal atom much more strongly than the other fluorenyl atoms. As a consequence, the η^5 coordination of type **A** often shows a clear tendency to asymmetry, with a metal slippage towards the bridgehead atom, i.e. towards the η^3 coordination of type **B**. It follows that the energy profile of the pathway connecting types **A** and **B** is particularly flat. For the same metal, coordination types **A** and **B** or intermediate can be very close in energy, so that the definitive choice will be made by small perturbations such as crystal packing forces or steric interactions, for instance. Such a situation is rather surprising, owing to the fact that $C_{13}H_9^-$ provides the metal with different numbers of electrons depending on whether it is an η^5 or η^3 (6 and 4, respectively) fashion, at least formally.

Fluorenyl complexes of group 2 tend to form hypercoordinated and hypervalent molecules in which the ionic bonding is likely to be very important. Some participation to the bonding of the metal valence d orbitals could possibly exist for the heavier elements of this group [13]. In the case of the more covalent complexes of group 3, the most commonly encountered architecture is that containing the motif of the well-known stable 16-electron compounds of the type Cp_2ML_2 [16]. In this motif, the metal binds to the fluorenyl C_5 ring(s) either in the **A** or **B** form, depending on the nature of the compound. The particular stability of this architecture is demonstrated in several examples by the existence of an agostic interaction at the right place when only one L ligand is present in the metal coordination sphere. Other often-complicated structures have been characterized with group 3 metals, exhibiting various types of fluorenyl coordination modes. Most of them are electron-deficient, but a few are able to accommodate enough ligands in their coordination sphere for satisfying the 18-electron rule.

The chemistry of fluorenyl complexes of groups 2 and 3 obviously sets up challenges for both organometallic and computational chemists. The large variety of coordination modes provides opportunities to control the coordination sphere and saturation of the metal center, and the overall complex geometry. These factors, when approaching the usual limits (e.g. very narrow bite angles), can affect significantly the electronic properties of the metal site in complexes and

therefore the reactivity of the latter, making them interesting candidates for a variety of catalytic applications.

References

[1] (a) H.G. Alt, E. Samuel, Chem. Soc. Rev. 27 (1998) 323, and references therein;
(b) H.G. Alt, Macromol. Symp. 173 (2001) 65.
[2] (a) J.A. Ewen, R.L. Jones, A. Razavi, J. Am. Chem. Soc. 110 (1988) 6255;
(b) A. Razavi, V. Bellia, Y.D. De Brauwer, K. Hortmann, L. Peters, S. Sirol, S. Van Belle, U. Thewalt, Macromol. Chem. Phys. 205 (2004) 347.
[3] S.A. Miller, J.E. Bercaw, Organometallics 23 (2004) 1777.
[4] H. Jiao, P. von, R. Schleyer, Y. Mo, M.A. McAllister, T.T. Tidwell, J. Am. Chem. Soc. 119 (1997) 7075.
[5] K. Yoshizawa, K. Yahara, A. Taniguchi, T. Yamabe, T. Kinoshita, K. Takeuchi, J. Org. Chem. 64 (1999) 2821.
[6] H. Elouni, S. Kahlal, J.-F. Carpentier, J.-Y. Saillard, unpublished results.
[7] R.D. Shannon, Acta Crystallogr. A 32 (1976) 751.
[8] (a) C. Eaborn, P.B. Hitchcock, K. Izod, Z.-R. Lu, J.D. Smith, Organometallics 15 (1996) 4783;
(b) K. Izod, W. Clegg, S.T. Liddle, Organometallics 19 (2000) 3640.
[9] I.L. Fedushkin, T.V. Petrovskaya, M.N. Bochkarev, S. Dechert, H. Schumann, Angew. Chem. Int. Ed. 40 (2001) 2474.
[10] T.E. Hogen-Esch, J. Smid, J. Am. Chem. Soc. 91 (1969) 4580.
[11] T.E. Hogen-Esch, J. Smid, J. Am. Chem. Soc. 94 (1972) 9240.
[12] U. Takaki, J. Smid, J. Am. Chem. Soc. 96 (1974) 2588.
[13] G. Mosges, F. Hampel, P.R. Schleyer, Organometallics 11 (1992) 1769.
[14] M. Schlosser, in: M. Schlosser (Ed.), Organometallics in Synthesis – A Manual, Wiley, Chichester, 2002, pp. 1–352.
[15] W.J. Evans, T.S. Gummerscheimer, T.J. Boyle, J.W. Ziller, Organometallics 13 (1994) 1281.
[16] (a) T.A. Albright, J.K. Burdett, M.-H. Whangbo, Orbital Interactions in Chemistry, Wiley, New York, 1985;
(b) J.W. Lauher, R. Hoffmann, J. Am. Chem. Soc. 98 (1976) 1729.
[17] A.A. Trifonov, E.N. Kirillov, S. Dechert, H. Schumann, M.N. Bochkarev, Eur. J. Inorg. Chem. (2001) 2509.
[18] A.A. Trifonov, E.A. Fedorova, G.K. Fukin, N.O. Druzhkov, M.N. Bochkarev, Angew. Chem. Int. Ed. 43 (2004) 5045.
[19] H. Nakamura, Y. Nakayama, H. Yasuda, T. Maruo, N. Kanehisa, Y. Kai, Organometallics 19 (2000) 5392.
[20] P. Kubacek, R. Hoffmann, Z. Havlas, Organometallics 1 (1982) 180, and Ref. [6] in this paper.
[21] S.Ya. Knjazhanski, L. Elizalde, G. Cadenas, B.M. Bulychev, J. Organomet. Chem. 568 (1998) 33.
[22] S.Ya. Knjazhanski, L. Elizalde, G. Cadenas, B.M. Bulychev, J. Polym. Sci. A: Polym. Chem. 36 (1998) 1599.
[23] S. Harder, F. Feil, T. Repo, Chem. Eur. J. 8 (2002) 1991.
[24] S. Harder, Angew. Chem. Int. Ed. 43 (2004) 2714.
[25] F. Feil, S. Harder, Eur. J. Inorg. Chem. (2003) 3401.
[26] R. Littger, H. Noth, M. Wagner, Chem. Ber. 127 (1994) 1901.
[27] S. Harder, M. Lutz, A.W.G. Straub, Organometallics 16 (1997) 107.
[28] E.D. Brady, T.P. Hanusa, M. Pink, V.G. Young, Inorg. Chem. 39 (2000) 6028.
[29] J.J. Eisch, R. Sanchez, J. Organomet. Chem. 296 (1985) 27.
[30] H. Viebrock, D. Abeln, E. Weiss, Z. Naturforsch. Teil B 49 (1994) 89.
[31] K.A. Allan, B.G. Gowenlock, W.E. Lindsell, J. Organomet. Chem. 65 (1974) 1.
[32] S. Harder, F. Feil, K. Knoll, Angew. Chem. Int. Ed. 40 (2001) 4261.
[33] F. Feil, C. Muller, S. Harder, J. Organomet. Chem. 683 (2003) 56.
[34] S. Harder, F. Feil, Organometallics 21 (2002) 2268.
[35] L.F. Rybakova, A.B. Sigalov, O.P. Syutkina, E.N. Egorova, I.P. Beletskaya, Izv. Akad. Nauk SSSR Ser. Khim. (1981) 2415.
[36] A.B. Sigalov, L.F. Rybakova, O.P. Syutkina, R.L. Shifrina, Yu.S. Bogachev, I.L. Zhuravleva, I.P. Beletskaya, Izv. Akad. Nauk SSSR Ser. Khim. (1983) 918.
[37] R. Taube, H. Windisch, J. Organomet. Chem. 472 (1994) 71.
[38] C. Qian, W. Nie, J. Sun, J. Chem. Soc., Dalton Trans. (1999) 3283.
[39] C. Qian, W. Nie, J. Sun, J. Organomet. Chem. 626 (2001) 171.
[40] C. Qian, W. Nie, Y. Chen, J. Sun, J. Organomet. Chem. 645 (2002) 82.
[41] A.K. Dash, A. Razavi, A. Mortreux, C.W. Lehmann, J.-F. Carpentier, Organometallics 21 (2002) 3238.
[42] E. Kirillov, L. Toupet, C.W. Lehmann, A. Razavi, S. Kahlal, J.-Y. Saillard, J.-F. Carpentier, Organometallics 22 (2003) 4038.
[43] E. Kirillov, C.W. Lehmann, A. Razavi, J.-F. Carpentier, Organometallics 23 (2004) 2768.
[44] E. Kirillov, C.W. Lehmann, A. Razavi, J.-F. Carpentier, J. Am. Chem. Soc. 126 (2004) 12240.
[45] M.-H. Lee, J.-W. Hwang, Y. Kim, J. Kim, Y. Han, Y. Do, Organometallics 18 (1999) 5124.
[46] C. Qian, W. Nie, J. Sun, Organometallics 19 (2000) 4134.
[47] C. Qian, W. Nie, Y. Chen, J. Sun, J. Organomet. Chem. 647 (2002) 114.
[48] M.F. Llauro, C. Monnet, F. Barbotin, V. Monteil, R. Spitz, C. Boisson, Macromolecules 34 (2001) 6304.
[49] J. Eppinger, M. Spiegler, W. Hieringer, W.A. Hermann, R. Anwander, J. Am. Chem. Soc. 122 (2000) 3080.
[50] E. Kirillov, L. Toupet, C.W. Lehmann, A. Razavi, J.-F. Carpentier, Organometallics 22 (2003) 4467.
[51] E. Kirillov, C.W. Lehmann, A. Razavi, J.-F. Carpentier, Eur. J. Inorg. Chem. (2004) 943.
[52] Z. Hou, C. Yoda, T. Koizumi, M. Nishiura, Y. Wakatsuki, S. Fukuzawa, J. Takats, Organometallics 22 (2003) 3586.
[53] (a) Z. Hou, Y. Wakatsuki, Coord. Chem. Rev. 231 (2002) 1;
(b) J. Gromada, J.-F. Carpentier, A. Mortreux, Coord. Chem. Rev. 248 (2004) 397;
(c) H. Yasuda, J. Organomet. Chem. 647 (2002) 128.
[54] (a) G.A. Molander, J.A.C. Romero, Chem. Rev. 102 (2002) 2161;
(b) S. Hong, T.J. Marks, Acc. Chem. Res. 37 (2004) 673.
[55] W.J. Evans, H. Katsumata, Macromolecules 27 (1994) 4011.
[56] E.N. Kirillov, E.A. Fedorova, A.A. Trifonov, M.N. Bochkarev, Appl. Organomet. Chem. 15 (2001) 151.
[57] F. Feil, S. Harder, Macromolecules 36 (2003) 3446.
[58] K.C. Hultzsch, P. Voth, K. Beckerle, T.P. Spaniol, J. Okuda, Organometallics 19 (2000) 228.
[59] (a) V. Monteil, R. Spitz, F. Barbotin, C. Boisson, Macromol. Chem. Phys. 205 (2004) 737;
(b) C. Boisson, V. Monteil, J. Thuilliez, R. Spitz, C. Monnet, M.-F. Llauro, F. Barbotin, P. Robert, Macromolecular Symposia, in press, and references therein.
[60] A.K. Dash, T.J. Marks, E. Kirillov, J.-F. Carpentier, unpublished results.